Journal of Infection 79 (2019) 139–152

Contents lists available at ScienceDirect

Journal of Infection

journal homepage: www.elsevier.com/locate/jinf

ESAT-6 modulates Calcimycin-induced autophagy through microRNA-30a in mycobacteria infected macrophages

Assirbad Behura[a], Abtar Mishra[a], Saurabh Chugh[b], Shradha Mawatwal[a], Ashish Kumar[a], Debraj Manna[a], Amit Mishra[c], Ramandeep Singh[b], Rohan Dhiman[a,*]

[a] Laboratory of Mycobacterial Immunology, Department of Life Science, National Institute of Technology, Rourkela 769008, Odisha, India
[b] Tuberculosis Research Laboratory, Vaccine and Infectious Disease Research Centre, Translational Health Science and Technology Institute, NCR Biotech Science Cluster, 3rd Milestone, Faridabad-Gurugram Expressway, PO Box # 4, Faridabad 121001, Haryana, India
[c] Cellular and Molecular Neurobiology Unit, Indian Institute of Technology Jodhpur, Rajasthan 342011, India

ARTICLE INFO

Article history:
Accepted 3 June 2019
Available online 8 June 2019

Keywords:
Autophagy
Calcimycin
ESAT-6
Human macrophages
micro-RNA
Tuberculosis

SUMMARY

Objective: *Mycobacterium tuberculosis* (*M. tb*) has a sumptuous repertoire of effector molecules to counter host defenses. Some of these antigens inhibit autophagy but the exact mechanism of this inhibition is poorly understood.
Methods: Purified protein derivative (PPD) was fractionated using 10 (PPD 10, antigenic molecular weight > 10 kDa) and 3 (PPD 3, mol. weight > 3 kDa) kDa cutters. Effect of these fractions on Calcimycin-induced autophagy and intracellular mycobacterial viability was then studied using different experimental approaches.
Result: We found significant downregulation of autophagy by PPD 3 pre-treatment in Calcimycin-treated dTHP-1 cells compared to PPD 10. This reduction in autophagy also corroborated with the enhanced survival of mycobacteria in macrophages. We demonstrate that recombinant early secreted antigenic target 6 (rESAT-6) is responsible to inhibit Calcimycin-induced autophagy and enhance intracellular survival of mycobacteria. We also show that pre-treatment with rESAT-6 upregulates microRNA (miR)-30a-3p expression and vis-a-vis downregulates miR-30a-5p expression in Calcimycin-treated dTHP-1 cells. Transfection studies with either miR-30a-3p inhibitor or miR-30a-5p mimic clearly elucidated the opposing roles of miR-30a-3p and miR-30a-5p in rESAT-6 mediated mycobacterial survival through autophagy inhibition.
Conclusion: Taken together, our result evidently highlights that rESAT-6 enhances intracellular survival of mycobacteria by modulating miR-30a-3p and miR-30a-5p expression.

Introduction

In spite of putting in tremendous efforts to eradicate Tuberculosis (TB) by many stakeholders, this disease is still the leading killer among infectious diseases that have caused enormous affliction to humanity. As per the latest global TB report 2018 by World Health Organization (WHO), TB has impacted 10.0 million people in 2017 and 1.6 million succumb to this deadly demon.[1] All efforts to make this world TB-free have yielded limited results due to the emergence of multidrug-resistant (MDR) and extremely drug-resistant (XDR) strains of *Mycobacterium tuberculosis* (*M. tb*). Above that, poor efficacy of *M. bovis* BCG, the only available vaccine till date against TB has made the situation more precarious.[2,3] Therefore, rejuvenation of our approaches especially host-pathogen interaction is urgently required to lessen the ever-growing threat of TB.

M. tb intrudes the host through respiratory route and establishes a successful infection inside the alveolar macrophages.[4,5] These macrophages inhibit the *M. tb* growth intracellularly by employing diverse array of strategies to elicit phagocytosis of *M. tb* through surface receptors, phagosome lysosome fusion, generation of reactive oxygen and nitrogen intermediates (ROI and RNI),

Abbreviations: M. bovis BCG, *Mycobacterium bovis* BCG; *M. tb*, *Mycobacterium tuberculosis*; *M. smegmatis*, *Mycobacterium smegmatis*; TB, Tuberculosis; dTHP-1, differentiated THP-1; PPD, Purified Protein Derivative; MDR, Multidrug-resistant; XDR, Extremely drug-resistant; rESAT-6, Recombinant early secreted antigenic target; miR, microRNA; ROI, Reactive oxygen intermediates; RNI, Reactive nitrogen intermediates; *Eis*, Enhanced intracellular survival; ManLAM, Mannose-capped lipoarabinomannan; PtpA, Phosphotyrosyl phosphatase activator; ESX-1, ESAT-6 secretion system-1; CFP-10, Culture filtrate protein of 10 kDa; Atg, Autophagy-related gene; LC3, Microtubule-associated protein 1A/1B-light chain 3; PMA, Phorbol 12-myristate 13-acetate; 3-MA, 3-Methyladenine; Baf-A1, Bafilomycin A1; MDC, Monodansylcadaverine; qRT-PCR, Quantitative Real-time PCR; mRFP, Monomeric red fluorescent protein; EGFP, Enhanced green fluorescent protein; HDT, Host-directed therapy.

* Corresponding author.
E-mail address: dhimanr@nitrkl.ac.in (R. Dhiman).

https://doi.org/10.1016/j.jinf.2019.06.001
0163-4453/

innate and adaptive immune mechanisms and effector mechanisms like apoptosis and autophagy.[6–10] Autophagy is a well-conserved degradative process that maintains intracellular homeostasis by generating double membrane envelope bodies called as autophagosome that fuses with the lysosomes to deliver its intracellular milieu.[11–13] The autophagosome genesis is highly complex and regulated by autophagy-related proteins (ATG) which are categorized into six complexes namely: ULK1 (Unc-51-like kinase 1) complex, ATG 9, class III PI3K (PI3KC3) complex, ATG 2-18 complex, ubiquitin (Ub)-like protein complex having covalent conjugation allies like Atg 12-Atg 5-Atg 16L and ATG 8 conjugation system.[13,14]

Numerous studies have highlighted the regulatory role of autophagy in progression of various diseases such as neurodegenerative disorders, cancer, autoimmune aberrations, muscular and heart ailments, aging and infectious diseases.[15] In infectious diseases, autophagy have been implicated in cellular pathways ranging from lymphocyte development, antigen presentation, antibody production to neutralizing pathogen[16–19] that contribute in killing intracellular pathogens including *M. tb*.[9,20–24] However, *M. tb* is able to evade autophagy by activating different mechanisms in host cells such as elevated secretion of Th2 compared to Th1 cytokines, inhibition of cytosolic Ca^{2+} production and abrogation of Rab7 recruitment on the autophagosomes.[25–33] In addition, *M. tb* genome encodes for several effector molecules such as enhanced intracellular survival (*Eis*) gene, mannose-capped lipoarabinomannan (ManLAM), protein tyrosine phosphatases (MptpA, MptpB) and ESAT-6 secretion system-1 (ESX-1) that modulates the host autophagic response for its survival intracellularly.[34–39] ESX-1 is a type VII secretion system encoded by the region of difference 1 (RD1) locus that is absent in avirulent strains and has been associated with *M. tb* virulence.[40–44] RD-1 locus includes two of the major immunodominant *M. tb* antigens, culture filtrate protein of 10 kDa (CFP-10) and ESAT-6.[45] ESAT-6 antagonizes the host defense system by inhibiting phagosome maturation, translocation of *M. tb* to the cytosol, impeding T cell responses, augmenting host cell apoptosis for *M. tb* spreading and inducing secretion of Type 1 interferons.[46] There have been conflicting reports highlighting autophagy induction or inhibition potential of ESAT-6 in mycobacteria infected macrophages.[37,47] However, the major consensus in the field is that ESAT-6 is beneficial for *M. tb* survival by suppressing autophagy.[48] Previously, it has also been demonstrated that ESAT-6 modulates autophagy by upregulating microRNA (miR)-155 expression.[49] miRNAs are short chain of nucleotides of approximate 22-mer length and known to epigenetically control gene expression by binding to 3′ untranslated regions (UTRs) of target mRNAs.[50] miRNAs regulate different cellular processes ranging from metabolism to immunity including autophagy in TB.[51] It has been shown that the expression of miR-17-5p, miR-27a, miR-30a, miR-33, miR-125a-3p, miR-144, miR-146a, miR-155 and miR-223 are modulated upon *M. tb* infection[52–62] but the exact mechanism of this regulation is not completely known. Recently we have shown that Calcimycin, a calcium ionophore inhibits intracellular avirulent mycobacterial growth in dTHP-1 cells by inducing autophagy through the interplay of intracellular calcium level and IL-12.[23,24]

In the present study, we attempted to evaluate if mycobacterial antigens inhibit Calcimycin-induced autophagy through modulation of miRNA expression in macrophages. We observed that low molecular weight PPD fraction (3–10 kDa) could abrogate Calcimycin-induced autophagy and enhanced intracellular mycobacterial viability. This abrogation was rESAT-6-dependent and resulted in altered expression of miR-30a-3p and miR-30a-5p. Interestingly, miR-30a-5p favored the host by eliciting autophagy upon Calcimycin treatment. We also demonstrate that rESAT-6 downregulated miR-30a-5p expression to enable mycobacteria for establishing infection in macrophages. Finally, transfections with either miR-30a-3p inhibitor or miR-30a-5p mimic in Calcimycin-treated cells upon rESAT-6 pre-treatment validated the dual strategy employed by mycobacteria to inhibit host anti-microbial pathways for its benefit.

Materials and methods

Cell culture and reagents

Maintenance of THP-1, the human monocyte cell line was done as described previously.[24] Phorbol 12-myristate 13-acetate (PMA) was used to differentiate THP-1 cells into macrophages as detailed earlier[24] and named as differentiated THP-1 (dTHP-1) cells. Amicon Ultra-15 centrifugal units having 10 kDa and 3 kDa cut off were bought from Merck KGaA (Darmstadt, Germany). Cell viability reagents like MTT cell assay kit and Trypan blue were procured from HiMedia Laboratory (Mumbai, India). Western blotting detection ECL kit was ordered from GE Healthcare (UK). All the primary antibodies (anti-[Beclin-1, Atg 7, LC3, Atg 3 and β-actin]) and secondary antibody (rabbit anti-HRP) were procured from Cell Signaling Technology (MA, USA). Special chemicals and kits like Bafilomycin A1 (Baf-A1), Calcimycin, Monodansylcadaverine (MDC), 3-methyl adenine (3-MA), Protease inhibitor cocktail (100 ×) and BCA protein estimation kit were supplied by Sigma (St. Louis, MO, USA). Mycobacterial growth media like Middlebrook (7H9 broth, 7H10 agar, 7H11 agar, ADC and OADC) were procured from BD (MD, USA). microRNA (miRNA or miR) primers were synthesized by Sigma (Bangalore, India). miRNA mimics, inhibitors and negative control were procured from Qiagen (Hilden, Germany). HiMedia Laboratory (Mumbai, India) was the supplier of all the other general chemicals used in this study.

Bacteria and infection

M. smegmatis mc^2155, *M. bovis* BCG and *M. tb* H37Rv were cultured and maintained for the infection experiments as described previously.[24,63] Protocol for infection experiments was also referred to the procedure published earlier.[24,63] In some of the combinations, dTHP-1 cells were transfected with miRNA mimics or inhibitors before infection with mycobacterial species. After infection, cells were overlaid with complete medium in the presence or absence of rESAT-6 or PPD.

PPD fractionation

The commercially available PPD was procured from AJ vaccines (Copenhagen, Denmark). This was concentrated using Amicon Ultra-15 centrifugal units having cut-off of either 10 or 3 kDa as per manufacturer's instructions. Briefly, concentrators were washed with 1 × PBS and 500 µl of PPD was loaded onto it. The contents were then centrifuged at 14,000 g for 5 min. at 4 °C and concentrated fraction was stored. The impurities were removed by washing the concentrated sample twice with 1 × PBS. The amount of protein in concentrated fraction was calculated using BCA method and stored as aliquots at −80 °C. The purity was analyzed by electrophoresing 40 µg of proteins on 15% native gel.

3-(4,5-Dimethylthiazol-2-yl)-2,5-diphenyltetrazolium bromide (MTT) assay

dTHP-1 cells were overlaid with medium containing different amounts of PPD for 24, 48 and 72 h and cell viability through MTT assay was measured as described previously.[23]

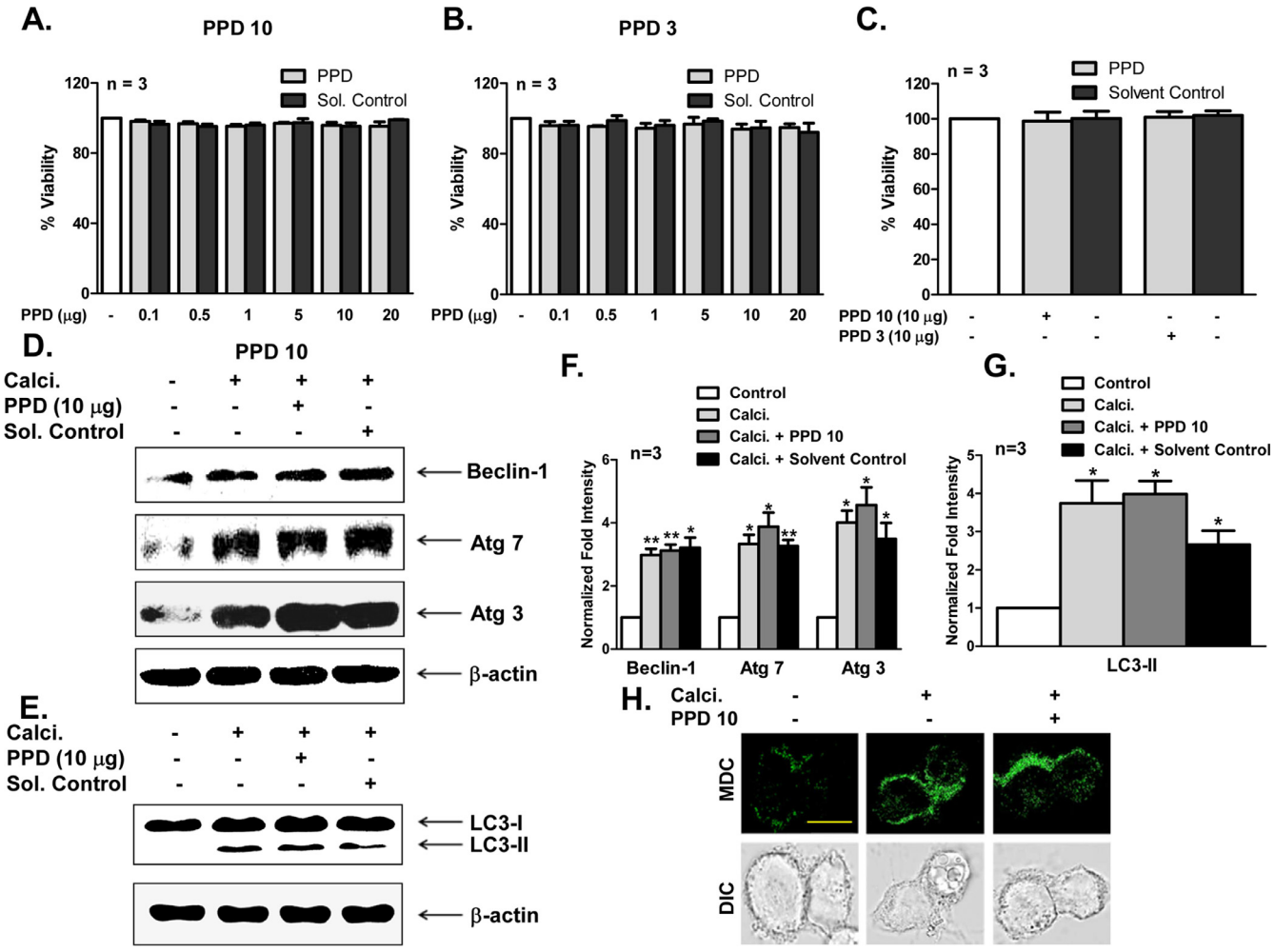

Fig. 1. Effect of pre-treatment of PPD 10 on cell viability and induction of autophagy by Calcimycin (Calci.) in dTHP-1 cells. A and B, dTHP-1 cells were incubated with different doses of either PPD 10 (A) or PPD 3 (B) for 72 h. Cell viability was then assessed through MTT assay. Data shown denotes the percentage of cell viability compared to control cells. (C) dTHP-1 cells were treated with 10 μg dose of either PPD 10 or PPD 3 in separate wells for 72 h. At the culmination, cells viability was assessed through trypan blue dye. Data shown depicts the percentage of cell viability compared to control cells. (D) and (E) Pre-treatment of dTHP-1 cells was accomplished with either 10 μg of PPD 10 or corresponding solvent for 2 h before Calci. addition. After incubation of 12 h, the experiment was terminated by preparing whole cell lysates. Protein expression in the lysates was analysed through western blotting. Blots provided are the representation of one experiment performed three times. (F) and (G) Quantitation depicts the fold differences in the expression of protein compared to controls of triplicate experiments whose representative blots are provided in (D) and (E). (H) Pre-treatment of dTHP-1 cells for 2 h with PPD 10 (10 μg) was followed by addition of Calci. for 12 h. MDC stained cells were washed, fixed and mounted using a mounting medium for scoping through confocal microscope. Images given are the representation of experiment performed in duplicate. Scale bar 10 μm. Data quantitation of this figure is shown as Mean ± SEM in all the panels. $p < 0.005$ and < 0.05 is represented as ** and *, respectively.

Trypan blue dye exclusion assay

Trypan blue dye exclusion assay was also performed to determine the cell viability of dTHP-1 cells in the presence of PPD using earlier described protocol.[23] Briefly, at the end of PPD treatment, dTHP-1 cells were harvested and mixed with trypan blue. Cell viability was calculated after counting the cells through hemocytometer.

Western blot analysis

The analysis of protein expression was performed by Western blotting as per the protocol described previously.[24] Briefly, whole cell lysates were prepared in radioimmunoprecipitation assay (RIPA) buffer containing protease inhibitors. The samples were fractionated through SDS-PAGE and followed by steps such as overnight transfer of the proteins on to the membrane, blocking of membranes and incubation with primary and secondary antibody. The bands were detected using ECL kit. ImageJ software (NIH, USA) was used to quantitate fold intensities of the bands compared to their respective controls.

Confocal microscopy for LC3 puncta visualization

LC3 puncta formation was visualized and quantitated through confocal microscopy as described earlier.[24] After experimental manipulation, cells were fixed in p-formaldehyde (4%). Following permeabilization, cells were stained by incubating with the respective antibodies. The stained cells were mounted and images were captured using confocal scanning laser microscope (CSLM) (Leica Microsystems, Wetzlar, Germany). LC3 positive puncta were counted manually in approx. 50 cells per combination of each experiment. In order to study autophagosome maturation, ptf-LC3 plasmid was transfected either alone or in combination with 10 nM of miRNA in 0.25×10^6 dTHP-1 cells. After transfections, cells were cultured as per experimental requirements by pre-treating with rESAT-6 or PPD 3 or PPD 10 before Calcimycin treatment. After incubation for 12 h, cells were fixed, mounted and scoped using CSLM as dis-

cussed above. Adobe Photoshop version 7 software (Adobe system) was then used to process the acquired images.

Determination of CFU

Enumeration of CFU was done using protocol published earlier.[23] Briefly, 100 µl of cell lysates after log dilution were plated on either Middlebrook 7H10 agar (*M. smegmatis*) or 7H11 agar with OADC (*M. bovis* BCG) plates. The colonies were counted on either 4th day or 4th week for *M. smegmatis* or *M. bovis* BCG, respectively.

Expression and purification of ESAT-6

BL21 (λDE3, p*lysS*) strain of *E. coli* was used for expression and purification studies as discussed before.[64] The strain was transformed with plasmid pMRLB.7 containing gene Rv3875 (protein ESAT-6) from *M. tb* which was obtained through BEI Resources, NIAID, NIH, USA. The transformed bacteria were cultured in LB medium at 37 °C and induction for protein expression was done at $OD_{600\ nm}$∼0.6 by adding 1 mM of isopropyl β-D galactopyranoside (IPTG) for overnight at 18 °C. Following induction, bacterial cells were pelleted, sonicated and $(His)_6$-tagged protein was purified by affinity chromatography using Nickel nitrilotriacetic acid (Ni-NTA) respectively as per manufacturer's suggestions (GE Healthcare, UK). The purification of rESAT-6 was confirmed by SDS-PAGE analysis. The purified fractions were dialyzed, concentrated and stored at −80 °C in aliquots till further use. In few experiments, required quantity of rESAT-6, according to the combinations was first heat-denatured at 100 °C for 10 min. before pre-treating dTHP-1 cells and named as HD-ESAT-6.

MDC staining

MDC staining was performed as published earlier.[24] Briefly, MDC stained cells were fixed followed by mounting and scoping using CSLM. The acquired images were finally processed for presentation using Adobe Photoshop software.

Quantitative real-time PCR (qRT-PCR) analysis

1.5×10^6 dTHP-1 cells in triplicates were overlaid with medium containing rESAT-6 for 2 h followed by Calcimycin treatment for 12 h. At the end of incubation, miRNA was isolated from the cells using mirVana miRNA isolation kit (Ambion, USA) as per manufacturer's instruction. In other experiment, miRNA was also isolated following above protocol after 24 h of infection from uninfected or *M. tb* H37Rv/*M. tb* H37Rv Δ ESAT-6 infected dTHP-1 cells. Isolated miRNA (0.25 µg) was then reverse transcribed using PCR starter kit (Qiagen, Hilden, Germany) and quantification of miRNA was performed through SYBR green (Qiagen, Hilden, Germany). The expression of miRNA's was quantified and normalized to the levels of U6 that was used as endogenous controls. The universal primer supplied with the above-mentioned kit was used as a reverse primer for all the miRNAs except for U6. The primers used for qPCR analysis were miR-30a-3p (F): 5-CTTTCAGTCGGATGTTTGC-3; miR-30a-5p (F): 5-TGTAAACATCCTCGACTGGAA-3; miR-33a-3p (F): 5-CAATGTTT CCACAGTGCATC-3; miR-33a-5p (F): 5-GTGCATTGTAGTTGCATTG-3; miR-33b-5p (F): 5-GTGCATTGCTGTTGCAT-3; miR-17-5p (F): 5-CAAAGTGCTTACAGTGCAGG TAG-3; miR-125a-3p (F): 5-ACAGGTGAGGTTCTTGGGA-3; U6 (F): 5-CTCGCTTCGG CAGCAGCACATATACT-3 and U6 (R) 5-ACGCTTCACGAATTTGCGTGTC-3.

Transfection with miRNA

Transfections to dTHP-1 cells with either mimics or inhibitors of miR-30a-3p and −5p and corresponding negative control were accomplished at a final concentration of 10 nM using reagents as per manufacturer's recommendations (Santa Cruz Biotechnology; CA, USA). At 24 h post-transfection, cells were washed and pre-treated with rESAT-6 before adding Calcimycin. At an appropriate time, samples were prepared for real-time PCR or confocal microscopy or CFU enumeration according to the protocol discussed above.

Transfection experiments involving ptf-LC3 were performed by mixing 500 ng of plasmid with Lipofectamine 3000 according to the manufacturer's protocol (Invitrogen). In some of the experiments, ptf-LC3 was co-transfected with either miRNA mimics/inhibitors or negative control. At 24 h post-transfection, cells were washed and pre-treated with either PPD 3 or rESAT-6 before adding Calcimycin. After 12 h, cells were fixed before scoping using CSLM. The acquired images were then processed through Adobe Photoshop software as stated above.

Statistical analysis

Results obtained are statistically represented as mean ± SE. Paired *t*-test was used to calculate the statistical significance between different combinations in the experiment. Results with *p* value less than 0.05 were considered statistically significant.

Results

Non-cytotoxic dose of PPD 10 did not alter the Calcimycin-induced autophagic pathway in dTHP-1 cells

To investigate the role of mycobacterial antigens in regulating autophagic machinery of the host for its advantage, we first fractionated PPD into two fractions namely high (PPD 10; antigens with molecular weight > 10 kDa) and low (PPD 3; antigens with molecular weight > 3 kDa) molecular weight fractions. The purity of the fractionated proteins was verified by native PAGE electrophoresis before proceeding for further experiments (Fig. S1). Next, we evaluated different doses of PPD 10 and PPD 3 for their cytotoxicity in dTHP-1 cells. As expected, we did not observe any cytotoxicity associated with different doses of either PPD 10 or PPD 3 in dTHP-1 cells till 72 h of exposure using MTT and Trypan blue dye exclusion assay (Fig. 1(A)–(C) and Fig. S2). 10 µg dose of PPD 10 was selected to study its effect on Calcimycin-induced autophagy because this dose has already been reported earlier in modulating the host immune responses.[65,66] As expected, we observed significant upregulation of autophagy markers (Beclin-1, Atg 7 and Atg 3) in dTHP-1 cells after incubation with Calcimycin. We also observed that pre-treatment with PPD 10 did not alter the expression patterns of these markers upon Calcimycin addition (Fig. 1(D) and (F)). We further validated findings of the previous experiment by western blotting and confocal microscopy to check LC3-II expression and autophagic vacuole formation through MDC staining respectively. As observed earlier, Calcimycin treatment led to significant upregulation of LC3-II expression suggestive of autophagy induction but PPD 10 pre-treatment did not show any effect (Fig. 1(E) and (G)). We also performed MDC staining in Calcimycin-treated dTHP-1 cells to observe the effect of PPD 10 pre-treatment on autophagic vacuoles formation. Calcimycin treatment resulted in the formation of autophagic vacuoles in dTHP-1 cells but PPD 10 pre-treatment did not reverse this phenomenon (Fig. 1(H)). These results evidently suggest the absence of effector molecules in PPD 10 fraction that regulates host autophagic pathway in mycobacterial infection.

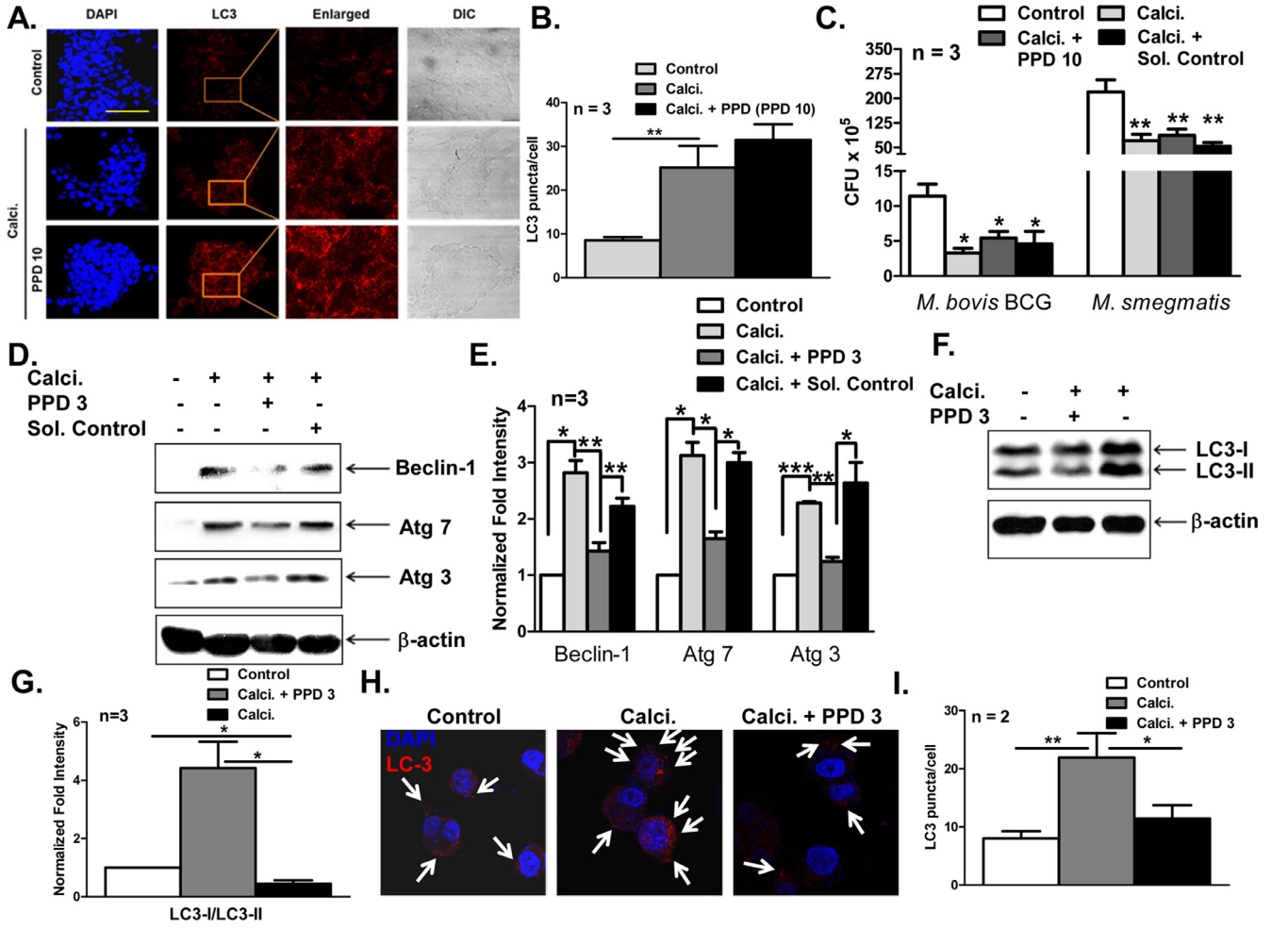

Fig. 2. Effect of the pre-treatment of PPD 10 (10 μg) on LC3 puncta formation and intracellular mycobacterial viability or PPD 3 (10 μg) on autophagy induction in Calcimycin (Calci.) treated dTHP-1 cells. (A) dTHP-1 cells were first given pre-treatment with PPD 10 before Calci. addition for 12 h. Upon completion, cells were immunostained with anti-LC3 antibody. Images of the stained cells were captured through confocal microscope. Experiments were performed three times and images provided are from one of them. Scale bar 50 μm. (B) LC3 puncta were counted from the random fields for quantification in different combinations of the experiment (representative image 2A). (C) *M. smegmatis* or *M. bovis* BCG infected dTHP-1 cells were treated with PPD 10 for 2 h before adding Calci. Later, cells were lysed, log diluted and spread on 7H10 (*M. smegmatis*) or 7H11 (*M. bovis* BCG) agar plates. CFUs for *M. smegmatis* or *M. bovis* BCG were counted on 4th day or 4th week respectively. (D) and (F) dTHP-1 cells were given pre-treatment with PPD 3 for 2 h before Calci. addition. After 12 h incubation, whole cell lysates were prepared and expression of autophagy marker proteins was checked through western blotting. Blots provided represent one experiment performed three times. (E) and (G) Quantitation of the triplicate experiments whose epresentative blots are shown in (D) and (F) depict the fold differences in the protein expression compared to controls. (H) Pre-treated dTHP-1 cells with PPD 3 were later incubated with Calci. for 12 h. At the completion, cells were stained with anti-LC3 antibody. Images of the stained cells were captured through confocal microscope. Images given are the representation of the experiment performed in duplicate. (I) Random fields taken during scoping (representative image 2H) were used to quantitate LC3 puncta in different combinations. Data quantitation of this figure is shown as Mean ± SEM in all the panels. $p < 0.001$, < 0.005 and < 0.05 is represented as ***, ** and *, respectively.

PPD 3 inhibited Calcimycin-induced autophagy in dTHP-1 cells compared to PPD 10

Since, LC3 quantitation through puncta formation is also regarded as a well-accepted approach to measure autophagy,[67] we next looked for LC3 puncta formation in Calcimycin-treated dTHP-1 cells pre-treated with PPD 10. As reported earlier, Calcimycin treatment led to significant LC3 puncta formation in dTHP-1 cells but pre-treatment with PPD 10 did not reverse this effect (Fig. 2(A) and (B)). As expected, PPD 10 pre-treatment also did not show any significant effect on the intracellular survival of slow- or fast-growing mycobacteria like *M. bovis* BCG or *M. smegmatis* respectively in the presence of Calcimycin (Fig. 2(C)). Next, we evaluated the potential of low molecular weight mycobacterial antigenic fraction like PPD 3 in modulating autophagy of Calcimycin-treated dTHP-1 cells. Interestingly, PPD 3 pre-treatment significantly decreased the expression of autophagy marker proteins by approximately 2.0 fold in Calcimycin-treated dTHP-1 cells in comparison to only treated cells (Fig. 2(D) and (E)). LC3-II expression through western blotting was also found to be significantly reduced by approximately 10.0 folds in Calcimycin-treated dTHP-1 cells pre-treated with PPD 3 compared to only treated cells without pre-treatment (Fig. 2(F) and (G)). These findings were also corroborated with confocal microscopy results where PPD 3 pre-treatment in Calcimycin-treated dTHP-1 cells specifically reduced LC3 puncta formation (Fig. 2(H)). These observations suggest that PPD 3 consists of several determinants that have the ability to inhibit Calcimycin-induced autophagy.

PPD 3 mediated abrogation of autophagic flux in Calcimycin-treated dTHP-1 cells affected the intracellular mycobacterial viability of M. smegmatis and M. bovis BCG

The autophagy inhibition potential of PPD 3 in Calcimycin-treated dTHP-1 cells was further verified through MDC staining. As expected, PPD 3 pre-treatment reduced autophagic vacuole formation in dTHP-1 cells treated with Calcimycin compared to the cells without pre-treatment (Fig. 3(A)) clearly implying the potential of

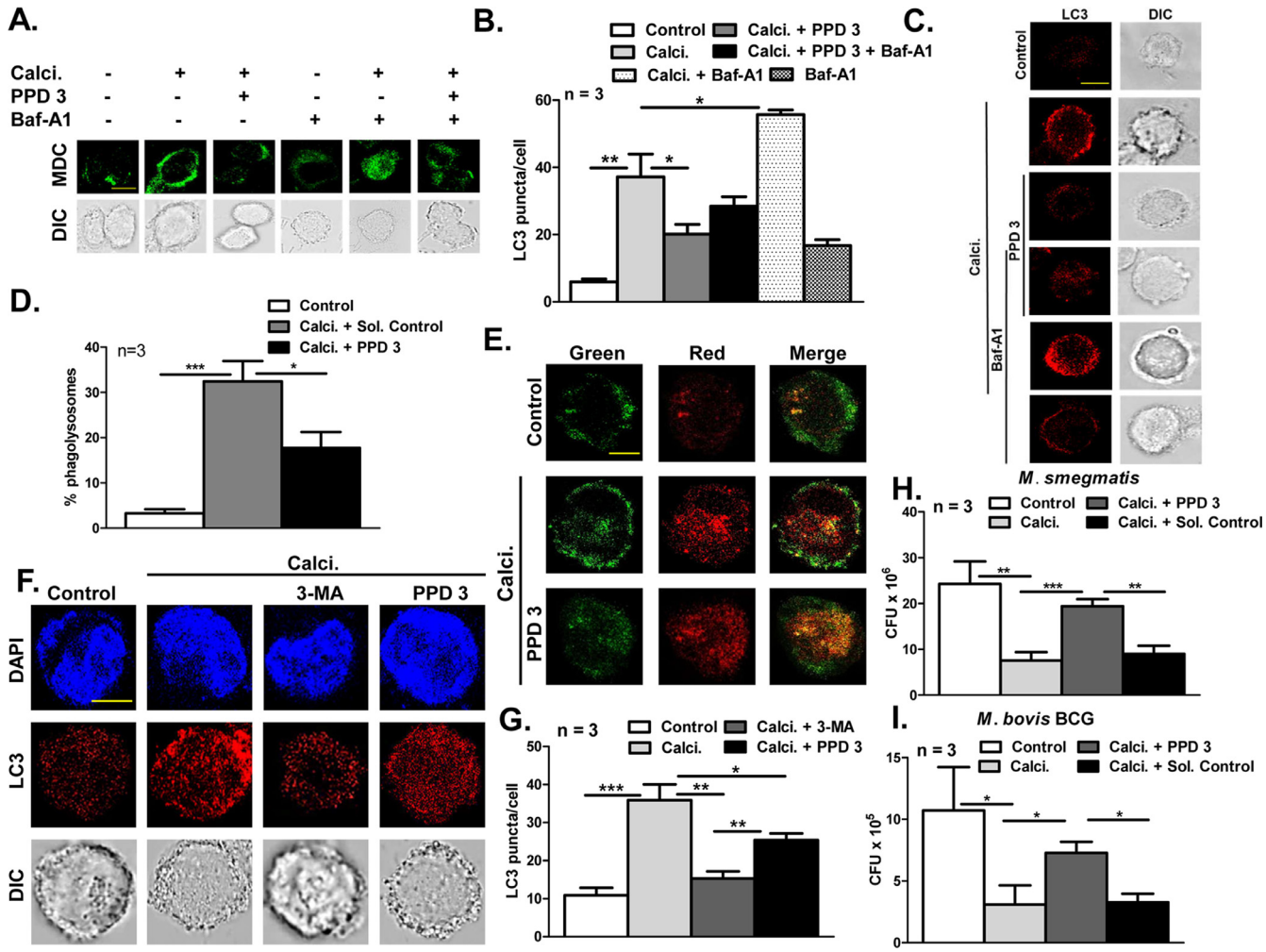

Fig. 3. PPD 3 (10 μg) pre-treatment in dTHP-1 cells treated with Calcimycin (Calci.) affect autophagic flux and intracellular mycobacterial viability. (A) Pre-treatment of dTHP-1 cells with PPD 3 was followed by Calci. addition. 3 h before the completion of incubation, some of the combinations were treated with Baf-A1. Later, MDC stained cells were fixed and mounted for visualization through a confocal microscope. Experiments were performed two times and images provided represent one of them. Scale bar 10 μm. (B) Random fields during microscopy (representative image 3C) were selected for counting LC3 puncta in all the combinations for quantification. (C) PPD 3 pre-treated dTHP-1 cells were incubated with Calci. for 12 h. Before completion of the incubation, Baf-A1 was added in few combinations. Later, cells were stained with LC3 antibody and visualized through microscopy. Images provided are from one experiment repeated three times. Scale bar 10 μm. (D) Pre-treatment of ptf-LC3 transiently transfected dTHP-1 cells with PPD 3 was followed by incubation with Calci. for 12 h. At the end, cells were mounted after fixation and images were captured through a confocal microscope. Random fields were selected (representative image 3E) for counting cells with phagosomes having co-localization of either red and green or only green fluorescence. (E) Images provided are the representation of one experiment performed in duplicate. Scale bar 10 μm. (F) dTHP-1 cells were pre-treated with 3-MA before adding PPD 3 followed by exposure to Calci. At the required time, cells were stained with anti-LC3 antibody after fixation and visualized through microscopy. Images provided are from one representative experiment performed in triplicate. Scale bar 10 μm. (G) Random fields during microscopy (representative image 3F) were selected for LC3 puncta quantitation in all the combinations. (H) and (I), dTHP-1 cells were infected with different mycobacteria like *M. smegmatis* (H) or *M. bovis* BCG (I) for indicated times, respectively. Then, some of the combinations were treated with either PPD 3 or solvent control before incubation with Calci. At indicated time points, cells were lysed and log dilutions were spread on 7H10 or 7H11 agar plates. *M. smegmatis* or *M. bovis* BCG CFUs were counted on 4th day or 4th week respectively. Data quantitation wherever given is shown as Mean ± SEM. $p < 0.001$, < 0.005 and < 0.05 is represented as ***, ** and *, respectively.

PPD 3 in inhibiting autophagic process in dTHP-1 cells. Since LC3 itself has been reported to be degraded by autophagy[68] so less autophagic vacuole or LC3 puncta formation can also be interpreted as an indicator of increased autophagy. In order to negate this possibility, autophagy flux experiment using vacuolar-type H+-ATPase inhibitor, Baf-A1 in the presence of PPD 3 in Calcimycin-treated dTHP-1 cells was performed.[69] Interestingly, no significant change in the number of autophagic vacuoles and LC3 puncta in Calcimycin-treated dTHP-1 cells upon PPD 3 pre-treatment was observed (Fig. 3(A)–(C)). This result clearly indicates the disruption of autophagic process by constituents of PPD 3 fraction in Calcimycin-treated dTHP-1 cells.

The propensity of a defective autophagic process by PPD 3 was further verified using tandem fluorescent tagged (ptf)-LC3 transiently transfected dTHP-1 cells as reported earlier.[70] We observed significant number of Calcimycin-treated dTHP-1 cells showing phagosomes with red fluorescence compared to phagosomes in PPD 3 pre-treated dTHP-1 cells with Calcimycin (Fig. 3(D) and (E)). This result verified the previous finding that PPD 3 inhibits autophagic flux in Calcimycin-treated dTHP-1 cells. Autophagy inhibition potency of PPD 3 was further compared with the known autophagy inhibitor like 3-MA. As expected, we observed that 3-MA is a better inhibitor of autophagy induced by Calcimycin in dTHP-1 cells compared to PPD 3 pre-treatment (Fig. 3(F) and (G)). This difference might be attributed to the purity and concentration of active antigen/s in total PPD 3 fraction in comparison to 3-MA. We further elucidated the effect of this inhibition by PPD 3 on the intracellular mycobacterial viability in dTHP-1 cells. We observed approximately 60% (7.6 ± 1.8 vs. 19.4 ± 1.5) and 58% (3.1 ± 1.5 vs. 7.3 ± 0.9) abrogation of the anti-mycobacterial effect

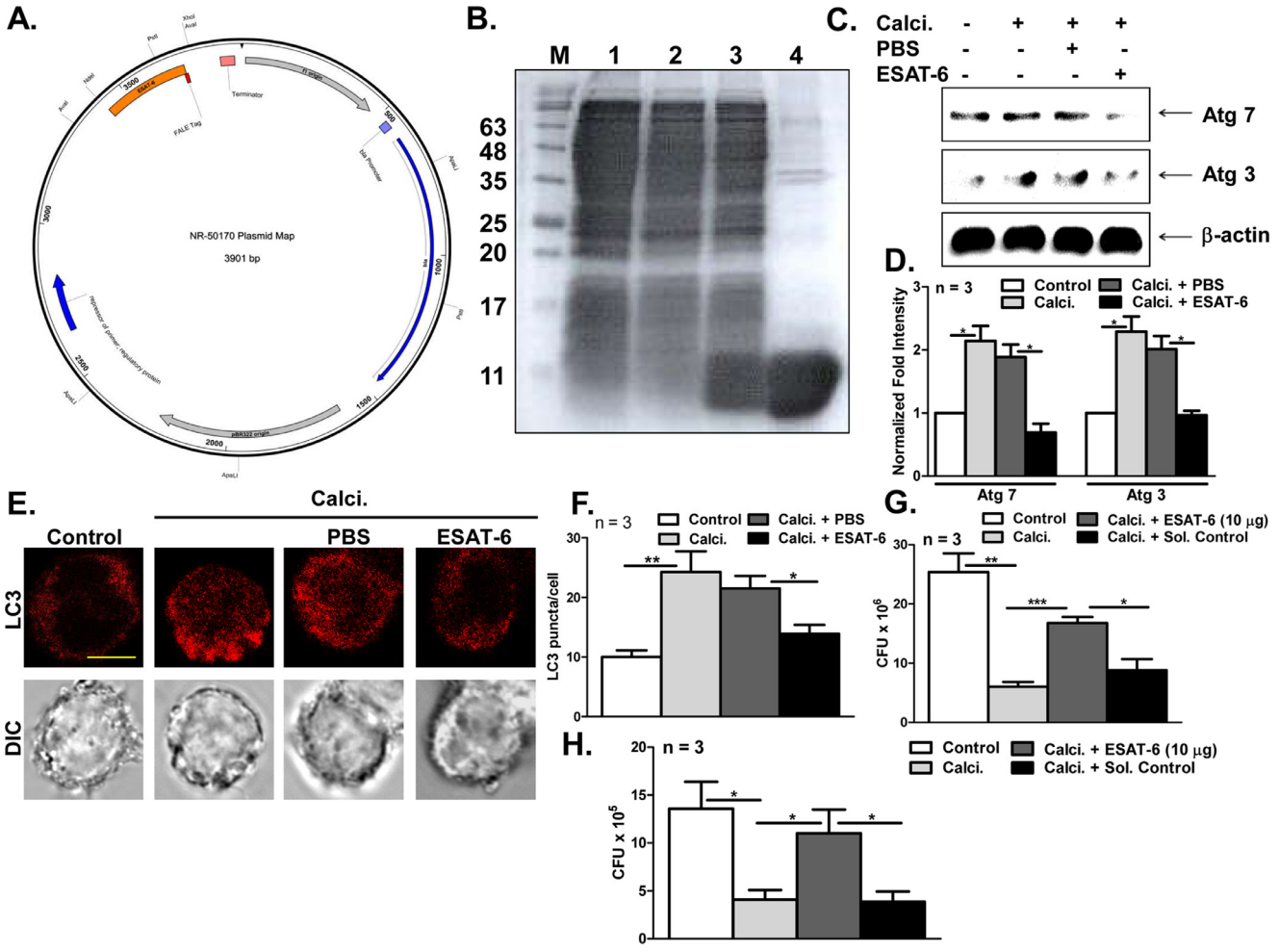

Fig. 4. Effect of purified rESAT-6 (10 μg) on autophagy and intracellular mycobacterial growth in dTHP-1 cells treated with Calcimycin (Calci.). (A) Map of the pMRLB.7 plasmid with *ESAT-6* gene. (B) *E. coli* BL21 (λDE3, p*lysS*) strain was transformed with pMRLB.7 and expression was induced by the addition of IPTG. Purity of the rESAT-6 was assessed through gel electrophoresis. M – Protein marker, 1 – Cells having pMRLB.7 with no *ESAT-6* gene, 2 – Uninduced cells with pMRLB.7 containing *ESAT-6* gene, 3 – Unpurified and induced cells containing pMRLB.7 with *ESAT-6* gene, 4 – Purified rESAT-6 protein. (C) dTHP-1 cells were pre-treated with rESAT-6 for 2 h before adding Calci. After 12 h, cell lysates were prepared and western blotting was performed. Blots shown are the representation that signifies the explained results of the experiment performed in triplicate. (D) Quantitation of the triplicate experiments whose representative blots are shown in (C) depicts the fold differences in the expression of test sample proteins compared to control. (E) rESAT-6 pre-treatment in dTHP-1 cells was followed by Calci. addition for 12 h. Later, cells were stained after fixation and imaged using a confocal microscope. Images provided are from the representative experiment performed three times. Scale bar 10 μm. (F) Random fields during microscopy (representative image 4E) were selected for LC3 puncta quantitation in all the combinations. (G) and (H) *M. smegmatis* (G) or *M. bovis* BCG (H) infected dTHP-1 cells were pre-treated with rESAT-6 before incubating with Calci. At indicated time points, prepared cells lysates were spread on 7H10 (*M. smegmatis*) or 7H11 (*M. bovis* BCG) agar plates after log dilution. Counting of CFUs was done on 4th day or 4th week for *M. smegmatis* or *M. bovis* BCG respectively. Data quantitation of this figure is shown as Mean ± SEM in all the panels. $p < 0.001$, < 0.005 and < 0.05 is represented as ***, ** and *, respectively.

of Calcimycin on intracellular survival of *M. smegmatis* (Fig. 3(H)) and *M. bovis* BCG (Fig. 3(I)) respectively on PPD 3 pre-treatment. These results categorically elucidate the enormous potential of mycobacterial antigens in hijacking the host responses for developing a congenial atmosphere intracellularly for mycobacteria to long term survival.

rESAT-6 in PPD 3 fraction inhibits autophagy and enhances intracellular mycobacterial survival in dTHP-1 cells upon Calcimycin treatment

ESAT-6, a major constituent of PPD 3 fraction has been shown to modulate many host responses like phagosome maturation.[45,46] Hence, we decided to study the role of ESAT-6 in inhibiting autophagy induced by Calcimycin in dTHP-1 cells. As described in methods, ESAT-6 was over-expressed in *E. coli* BL21 (λDE3, p*LysS*) strain (Fig. 4(A)). The recombinant protein was purified from clarified lysates using affinity chromatography and purity was verified through gel electrophoresis (Fig. 4(B)). Further, we used multi-parametric approaches to study the ability of rESAT-6 to inhibit autophagy in Calcimycin-treated dTHP-1 cells. We observed specific down-regulation of autophagy marker proteins like Atg 7 and Atg 3 in Calcimycin-treated dTHP-1 cells upon rESAT-6 pre-treatment (Fig. 4(C) and (D)). These observations implicate the role of rESAT-6 in imparting autophagy inhibition property in PPD 3 fraction. These results were further confirmed by determining LC3 puncta formation in Calcimycin-treated dTHP-1 cells with or without rESAT-6 pre-treatment. We observed significant downregulation of LC3 puncta formation in rESAT-6 pre-treated dTHP-1 cells before Calcimycin addition (Fig. 4(E) and (F)). Further, we also checked the basal effect of rESAT-6 on autophagy in dTHP-1 cells through LC3 puncta in the absence of Calcimycin treatment but no significant difference was observed between control and rESAT-6 added combinations in comparison to Calcimycin treated samples (Fig. S3A and B). Abrogation of autophagy by rESAT-6 also reversed the antimycobacterial effect of Calcimycin by 2.9 or 2.5 fold

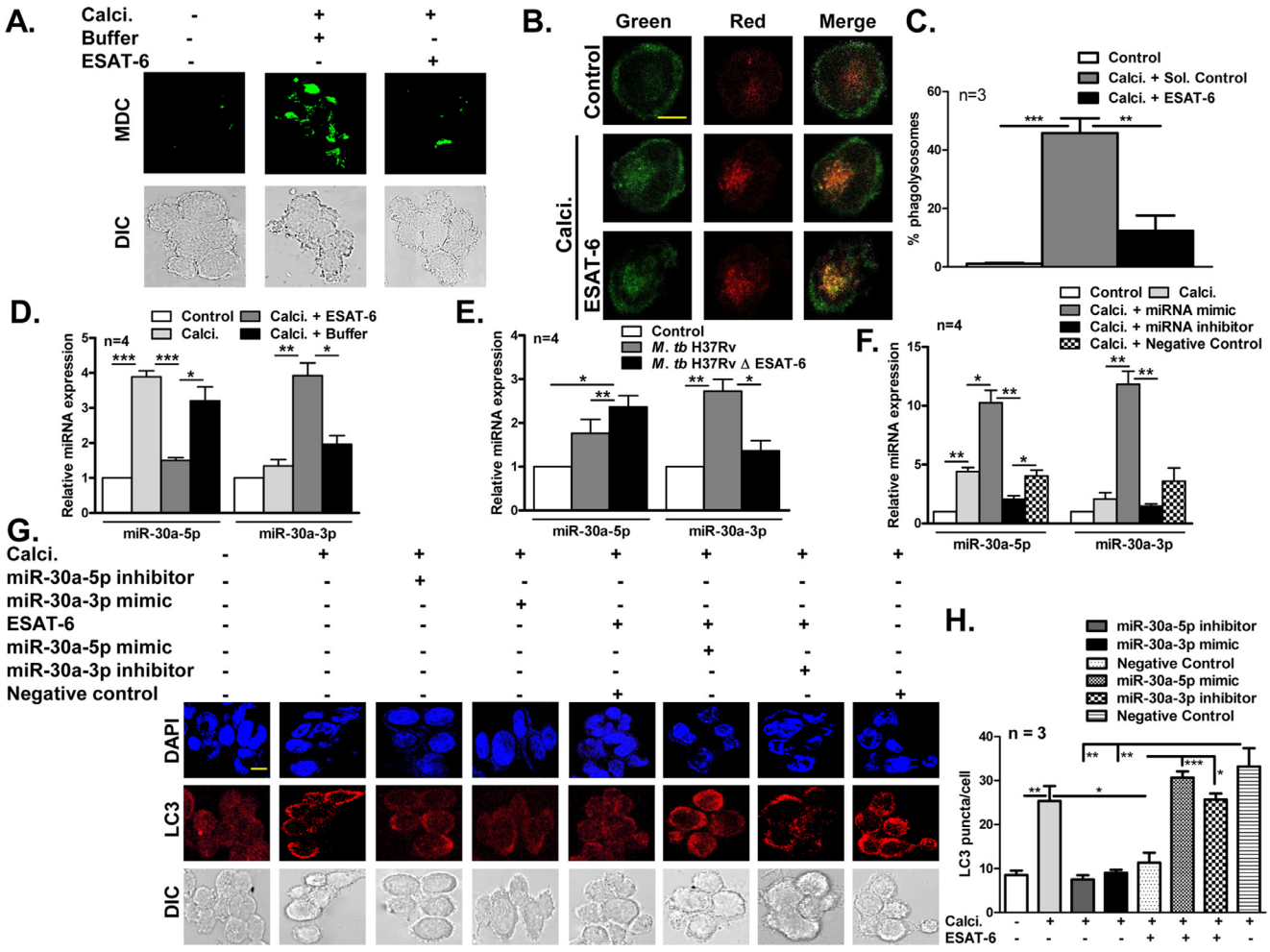

Fig. 5. Effect of rESAT-6 (10 μg) and miR-30a expression modulation on autophagic vacuole formation, miR-30a expression and autophagy respectively in Calcimycin (Calci.)-treated dTHP-1 cells. (A) rESAT-6 pre-treated dTHP-1 cells were incubated with Calci. for 12 h. MDC stained cells were then stained and analysed through a confocal microscope after fixation. Images provided are from representative experiment performed in duplicate. Scale bar 10 μm. (B) rESAT-6 pre-treatment in ptf-LC3 transfected dTHP-1 cells was followed by incubation with Calci. for 12 h. Cells were then fixed and visualized through a confocal microscope. Images provided are from one representative experiment performed in duplicate. Scale bar 10 μm. (C) Random fields were selected (representative image 5B) for counting cells with phagosomes having co-localization of either red and green or only green fluorescence. (D) miRNA from rESAT-6 pre-treated dTHP-1 cells incubated with Calci. was isolated and reverse transcribed. miRNA expression of miR-30a-5p and miR-30a-3p was quantified using SYBR green. Relative expression was calculated as fold difference after normalization with U6 as the internal control. (E) miRNA from uninfected and *M. tb* H37Rv or *M. tb* H37Rv Δ ESAT-6 infected cells was isolated after 24 h of infection. miRNA expression of miR-30a-5p and miR-30a-3p was quantified using SYBR green after reverse transcription as stated above. Relative expression as fold difference was calculated after normalization with U6 as the internal control. (F) Transfected dTHP-1 cells with either miRNA mimics or inhibitors were incubated with Calci. for 12 h. Later, miRNA expression was measured as detailed above. (G) Transfected dTHP-1 cells were pre-treated with rESAT-6 and later incubated with Calci. before staining with LC3 antibody. Images of the stained cells were captured using a confocal microscope after mounting the samples. Given images is the representation of an experiment performed in triplicate. Scale bar 10 μm. (H) Random fields during microscopy (representative image 5 G) were selected for quantitation of LC3 puncta in all the samples. Data quantitation of this figure is shown as Mean ± SEM in all the panels. $p < 0.001$, < 0.005 and < 0.05 is represented as ***, ** and *, respectively.

in *M. smegmatis* or *M. bovis* BCG infected dTHP-1 cells (Fig. 4(G) and (H)). Overall, these results are in concordance with the previously published reports that ESAT-6 suppresses host anti-microbial pathways such as autophagy that enables the bacteria to survive in macrophages.[37,48]

rESAT-6 inhibits Calcimycin-induced autophagy in dTHP-1 cells by modulating miR-30a expression

We further validated the autophagy inhibition potential of rESAT-6 in Calcimycin-treated dTHP-1 cells by MDC staining. As expected, clear autophagic vacuoles were observed in solvent control cells upon Calcimycin treatment but rESAT-6 pre-treatment reduced the formation of these vesicles in treated samples (Fig. 5(A)). On the other hand, rESAT-6 alone did not show any observable effect on basal autophagic vacuole formation compared to control cells (Fig. S3C). Transfection with ptf-LC3 also highlighted the inhibition of autophagic flux pathway by rESAT-6 in dTHP-1 cells treated with Calcimycin (Fig. 5(B) and (C)). These observations, confirm the role of ESAT-6 in interfering with the host's belligerent machinery during mycobacterial pathogenesis. Specificity of the inhibitory effect of ESAT-6 on autophagy was further confirmed by using HD-ESAT-6 that significantly enhanced the LC3 puncta formation, accumulation of autophagic vacuoles and protein expression of Beclin-1 and Atg 3 in Calcimycin-treated dTHP-1 cells in comparison to rESAT-6 pre-treated combination (Fig. S4). Several studies have predicted that miRNAs play an important role in regulating host responses during mycobacterial infection.[49,52] In order to understand the mechanism by which rESAT-6 inhibits Calcimycin-induced autophagy in dTHP-1 cells, we first checked the expression of various miRNAs like miR-30a-5p, miR-30a-3p, miR-33a-5p, miR-33a-3p, miR-33b-5p, miR-17-5p and miR-125a-3p that are reported to be involved in mycobacterial pathogenesis.[52] We observed that rESAT-6 pre-treatment specifically up-regulated

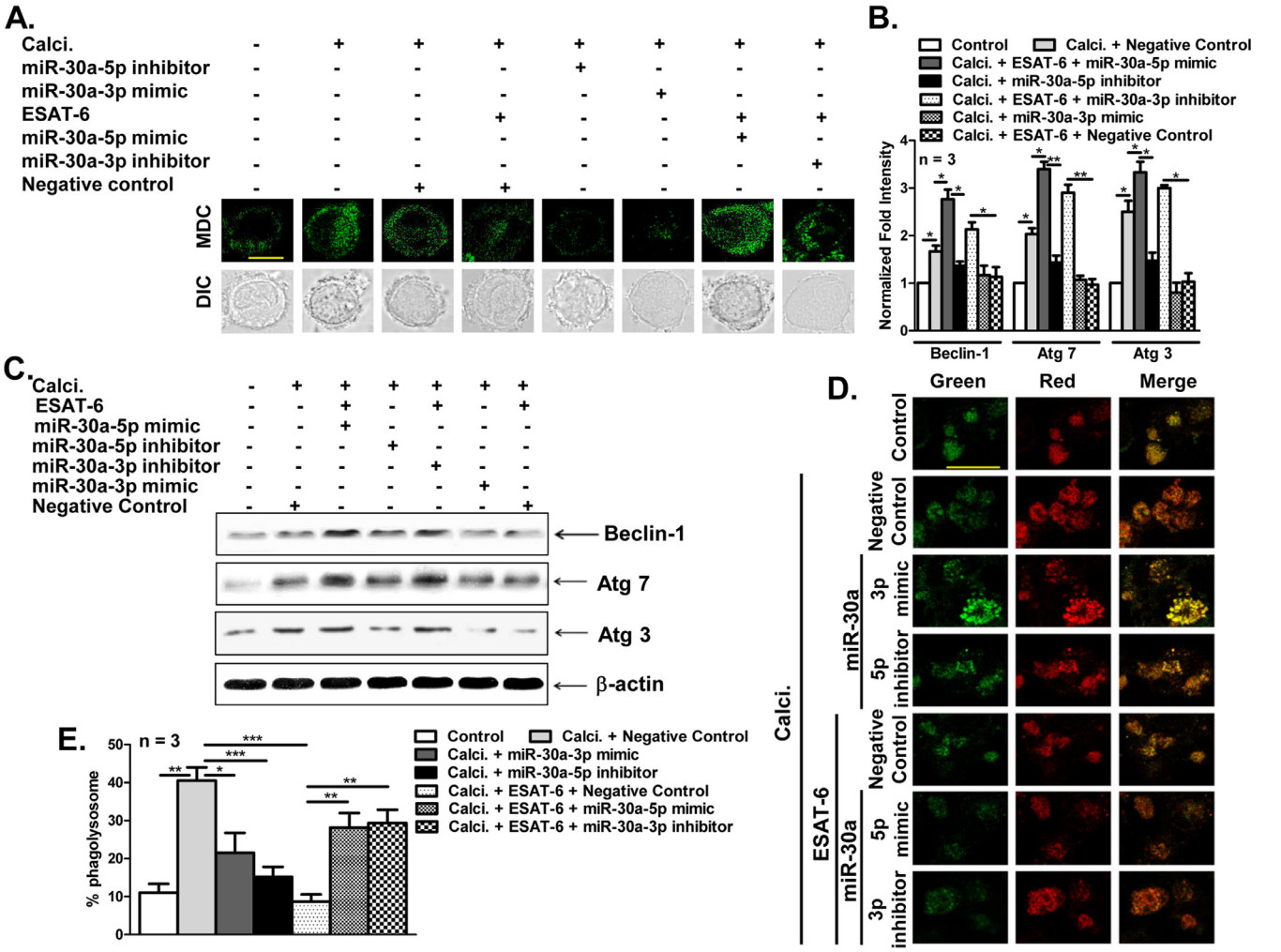

Fig. 6. Effect of the modulation of miR-30a expression on MDC staining and autophagy in dTHP-1 cells treated with Calcimycin (Calci.). (A) Transfected dTHP-1 cells were pre-treated with rESAT-6 (10 μg) followed by Calci. addition. After 12 h, MDC stained were analysed through a confocal microscope. Representative images of the experiment performed in duplicate are given. Scale bar 10 μm. (B) rESAT-6 (10 μg) pre-treatment in transfected dTHP-1 cells was followed by Calci. addition. Western blotting was performed with the prepared whole cell lysates. Quantitation of the triplicate experiments whose representative blots are shown in (C) depicts the fold differences in the protein expression compared to controls. (C) Western blot data is given in the form of representative blots of one experiment performed three times. (D) ptf-LC3 transfected and rESAT-6 (10 μg) pre-treated dTHP-1 cells were incubated with Calci. for 12 h. Fixed cells were visualized through a confocal microscope. Images given represent the experiment performed in triplicate. Scale bar 20 μm. (E) Random fields were selected (representative image 6D) for counting cells with phagosomes having co-localization of either red and green or only green fluorescence. Quantitative data wherever given in this figure is shown as Mean ± SEM. $p < 0.001$, < 0.005 and < 0.05 is represented as ***, ** and *, respectively.

miR-30a-3p by 3.0 fold and down-regulated miR-30a-5p by 2.6 fold in Calcimycin-treated dTHP-1 cells (Fig. 5(D)). We did observe some significant changes in the expression of miR-33a-3p, miR-17-5p and miR-125a-3p compared to other miRNAs upon rESAT-6 pre-treatment in Calcimycin-treated dTHP-1 cells (Fig. S5A) but since it was less compared to the expression of miR-30a-5p or miR-30a-3p, so for further mechanistic studies, we focused primarily on miR-30a-5p and miR-30a-3p. To further negate the possibility that modulation of miR-30a-5p and miR-30a-3p expression by rESAT-6 is non-specific, dTHP-1 cells were pre-treated with HD-rESAT-6 before adding Calcimycin. We found significant abrogation of the effect of rESAT-6 upon heat denaturation on miR-30a-5p and miR-30a-3p expression suggesting explicitly that ESAT-6 regulates expression of miR-30a-5p and miR-30a-3p (Fig. S5B). To deduce the physiological relevance of earlier result discussed in Fig. 5(D), expression of miR-30a-5p and miR-30a-3p was also measured in dTHP-1 cells infected with either *M. tb* H37Rv or *M. tb* H37Rv Δ ESAT-6 strains. We observed significant up-regulation of miR-30a-3p in *M. tb* H37Rv infected samples but not with *M. tb* H37Rv Δ ESAT-6 infection. On the contrary, miR-30a-5p was up-regulated by *M. tb* H37Rv Δ ESAT-6 infection in comparison to *M. tb* H37Rv challenge (Fig. 5(E)). To specifically pin-point the antagonistic role of miR-30a-5p and miR-30a-3p in Calcimycin-induced autophagy upon rESAT-6 pre-treatment, transfection experiments were performed using specific miRNA mimics and inhibitors to up-regulate and down-regulate the miRNA expression respectively. The specificity and effectivity of these mimics and inhibitors was confirmed through qPCR (Fig. 5(F)). The effect of these mimics and inhibitors on autophagy in Calcimycin-treated dTHP-1 cells was studied by observing LC3 puncta formation. As expected, we observed significantly more number of LC3 puncta in Calcimycin-treated dTHP-1 cells, but this number got reduced upon rESAT-6 pre-treatment (Fig. 5(G) and (H)). Interestingly, inhibitors against miR-30a-5p and miR-30a-3p individually abrogated the autophagy induction of Calcimycin and autophagy inhibition potency of rESAT-6 respectively (Fig. 5(G) and (H)). Alternatively, mimics against miR-30a-5p or miR-30a-3p reversed autophagy inhibition by rESAT-6 or autophagy induction by Calcimycin respectively

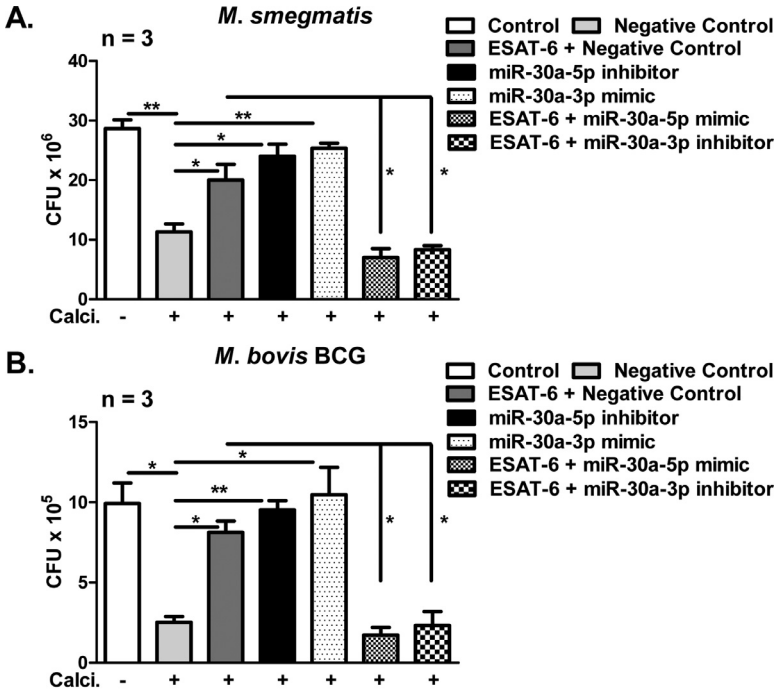

Fig. 7. Effect of the modulation of miR-30a on intracellular mycobacterial growth in dTHP-1 cells pre-treated with rESAT-6 (10 μg) before incubation with Calcimycin (Calci.). (A) and (B) dTHP-1 cells were firstly transfected transiently with mimics or inhibitors of miR-30a-3p and miR-30a-5p. Then, cells were infected with either *M. smegmatis* (A) or *M. bovis* BCG (B) before rESAT-6 pre-treatment. Cells were later incubated with Calci. and lysed either on 3rd (*M. smegmatis*, A) or 4th (*M. bovis* BCG, B) day post-infection. Serially diluted lysates were spread on 7H10 (*M. smegmatis*) or 7H11 (*M. bovis* BCG) agar plates. Quantification of the data is given as values represented in the form of Mean ± SEM. $p < 0.005$ and < 0.05 is represented as ** and *, respectively.

(Fig. 5(G) and (H)). These results clearly elucidated the antagonistic roles played by miR-30a-5p and miR-30a-3p in the modulation of autophagy in Calcimycin-treated dTHP-1 cells. Previous results were further verified through MDC staining where we observed less autophagic vacuoles in Calcimycin-treated dTHP-1 cells transfected with either miR-30a-3p mimic or miR-30a-5p inhibitor (Fig. 6(A)). Conversely, increased autophagic vacuole formation even in the presence of rESAT-6 after transfection with either miR-30a-3p inhibitor or miR-30a-5p mimic (Fig. 6(A)) clearly authenticate the earlier results that miR-30a variants like miR-30a-5p and miR-30a-3p play a monumental role in the regulation of autophagy by rESAT-6 in Calcimycin-treated dTHP-1 cells. Likewise, through western blotting, we observed a significant increase in the protein expression of autophagic markers like Beclin-1, Atg 7 and Atg 3 after treating the miR-30a-3p inhibitor or miR-30a-5p mimic transfected dTHP-1 cells with Calcimycin (Fig. 6(B) and (C)). These findings were further corroborated by studying autophagy flux in ptf-LC3 transfected dTHP-1 cells. We found either impaired or amplified autophagic flux in miR-30a-3p mimic and miR-30a-5p inhibitor or miR-30a-3p inhibitor and miR-30a-5p mimic transfected dTHP-1 cells in Calcimycin or Calcimycin + rESAT-6 combinations respectively (Fig. 6(D) and (E)). These results gave further credence to our findings that 3p and 5p mature forms of miR-30a originated from the same pre-miRNA precursor co-exist and show antagonism in regulating autophagy of Calcimycin-treated dTHP-1 cells in the presence or absence of rESAT-6.

Inhibition of miR-30a-3p dependent anti-autophagic response modulated by rESAT-6 curtails the intracellular mycobacterial survival

To correlate the previous results physiologically, expression levels of miR-30a-5p and miR-30a-3p were modulated intracellularly through transient transfection in dTHP-1 cells by using specific mimics or inhibitors against these miRNAs. Cells were later infected with either fast growing, *M. smegmatis* (Fig. 7(A)) or slow growing, *M. bovis* BCG (Fig. 7(B)) before incubating with rESAT-6 followed by Calcimycin treatment. As reported earlier, Calcimycin treatment reduced *M. smegmatis* survival intracellularly by 2.5 fold but this inhibition was abrogated by 1.8 or 2.1 or 2.2 fold upon rESAT-6 pre-treatment or miR-30a-5p inhibitor or miR-30a-3p mimic transfected dTHP-1 cells respectively (Fig. 7(A)). Interestingly, ability of rESAT-6 to favor *M. smegmatis* survival was arrested by 2.9 or 2.4 fold in miR-30a-5p mimic or miR-30a-3p inhibitor transfected dTHP-1 cells respectively (Fig. 7(A)). To physiologically relate the findings, an identical experiment was also performed with slow-growing mycobacterium, *M. bovis* BCG because of its similarity of 99.9% at nucleotide sequence level with pathogenic strain, *M. tb*.[71] Similar to the previous result, we found transfection with either miR-30a-5p inhibitor or miR-30a-3p mimic counterbalanced the inhibitory effect of Calcimycin on *M. bovis* BCG by 3.8 or 4.2 fold that was comparable to combination where rESAT-6 pre-treatment was given before Calcimycin addition (Fig. 7(B)). On the contrary, transfection with miR-30a-5p mimic or miR-30a-3p inhibitor neutralizes the effect of rESAT-6 by 4.8 and 3.5 fold respectively (Fig. 7(B)). These observations suggest the role of miR-30a-5p and miR-30a-3p in modulating rESAT-6 mediated mycobacterial survival in macrophages.

Overall, these results authoritatively delineate the fascinating novel facts of a survival strategy operated by mycobacteria through antigenic determinants like ESAT-6 that interferes in regulating miRNA-mediated autophagic response. To the best of our knowledge, this study for the first time mechanistically proves that rESAT-6 favors mycobacterial survival by selectively up-regulating miR-30a-3p vis-à-vis down-regulating miR-30a-5p, two different forms of same precursor miRNA, mir-30a that circumvents the hostilities like autophagy imposed by the host (Fig. 8).

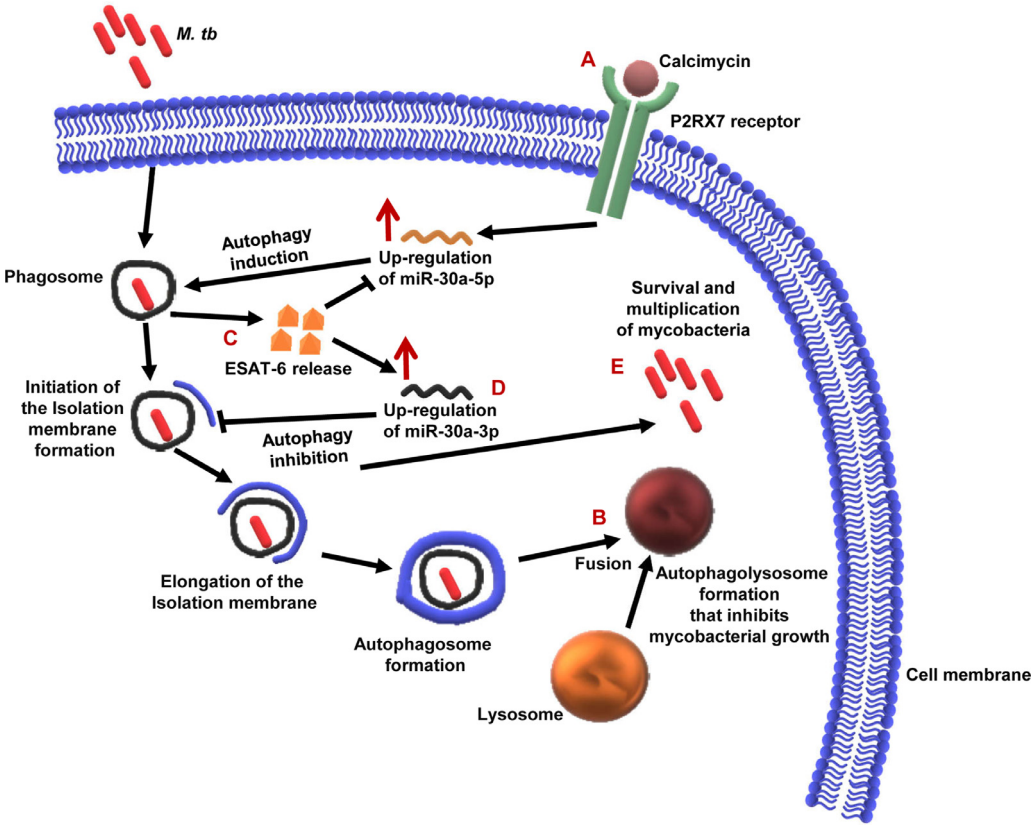

Fig. 8. Modulation of autophagy by rESAT-6 through miRNA in Calcimycin-treated and mycobacteria infected dTHP-1 cells. (A) Calcimycin treatment up-regulates miR-30a-5p in mycobacteria infected cells. (B) miR-30a-5p activation augments autophagy induction that ultimately leads to a decline in intracellular mycobacterial growth. (C) In spite of pressing conditions posed by the host, mycobacteria make pugnacious effort to circumvent these challenges by secreting dominant factors like ESAT-6. (D) rESAT-6 activates miR-30a-3p and also inhibits miR-30a-5p in Calcimycin-treated and mycobacteria infected dTHP-1 cells. (E) miR-30a-3p favours mycobacteria by inhibiting autophagosome maturation and ultimately inhibiting its fusion with the lysosome to offer survival advantage to the invading pathogen.

Discussion

In the last 2–3 decades, one of the landmark milestones that have transformed the concept of gene regulation and vis-à-vis central dogma is the discovery of miRNAs.[72] Since the pronouncement of their existence,[73] these single-stranded, non-coding RNAs of endogenous origin have been implicated in regulating diverse cellular processes like development, differentiation and homeostasis.[74] Published reports have highlighted the parallelism between anomalous miRNA expression and severity of disease progression in diabetes, macro and microvascular complications, kidney ailments, cancer and infectious diseases.[50,72,75,76] Recent studies that reported correlation between miRNA and its role in regulating immune responses during TB progression had given impetus to the potential of miRNAs to be used either as biomarker or host-directed therapy (HDT) to alleviate the disease burden.[56,77,78] We have previously deciphered the mechanistic pathways that govern the antimycobacterial role of Calcimycin through autophagy induction[23,24] but manipulation of Calcimycin-induced autophagy by mycobacteria and its antigens is not completely known to the best of our knowledge. So, the present study was undertaken to highlight the defense strategies used by mycobacteria or its associated antigen in suppressing the host barriers like autophagy and mechanism involved thereof, if any.

Since mycobacterial antigens have been reported to arrest functions of the immune cells like macrophages[79] so we first asked the question whether these antigens have any role in modulating the autophagy in Calcimycin-treated dTHP-1 cells. To specifically identify the antigen/s responsible for exerting its regulatory effect, two molecular weight fractions of PPD, PPD 10 and PPD 3 were fractionated. We observed that PPD 10 neither abrogated the autophagy induction potential of Calcimycin nor affected the intracellular survival of *M. smegmatis* or *M. bovis* BCG in dTHP-1 cells. Interestingly, PPD 3 pre-treatment partially rescued the Calcimycin-treated dTHP-1 cells from accomplishing autophagy that resulted in significant growth of intracellular mycobacteria thus highlighting the shrewd survival strategy executed by the bug for its longevity. One of the major reasons for partial reversal of Calcimycin's effect by PPD 3 can be credited to the concentration of specific antigen/s in this crude preparation that may be sub-optimal. The potency of PPD 3 compared to PPD 10 can be attributed to the low molecular weight of the antigens that preferentially aid their activation through pathways of degradation and processing leading to intracellular trafficking thus enhancing their regulatory responses.[80]

Previous studies have shown that ESAT-6 is one of the most prominent antigens in the low molecular weight fraction. The exact biological function of ESAT-6 either as a protective antigen or virulence factor is still under scrutiny.[81] Lately, emerging evidences from different groups have delineated the role of ESAT-6 in helping intracellular mycobacterial survival by suppressing autophagy.[37,48,82] These findings tempted us to speculate that ESAT-6 in PPD 3 may be a responsible factor in executing the inhibitory potential of PPD 3 against autophagy in Calcimycin-treated dTHP-1 cells. In support of our hypothesis, we observed that rESAT-6 pre-treatment significantly inhibited autophagy in Calcimycin-treated cells. This inhibition resulted in remarkable enhancement in the

intracellular growth of mycobacteria thus complementing the previously published results that have delineated the role of ESAT-6 in tilting the balance towards mycobacteria by suppressing host defenses.[37,48,82] The inefficiency of rESAT-6 to completely reverse the inhibitory effect of Calcimycin-induced autophagy makes strong case of a future study to investigate identification of other novel mycobacterial antigens that may regulate autophagy either individually or in combination with ESAT-6. Role of other mycobacterial antigens like CFP-10 in regulating the effector responses by ESAT-6 is also based on the published reports that have clearly elucidated the association between ESAT-6 and CFP-10, a responsible factor in controlling each other's stability, function and secretion.[81,83]

Next, we asked the pertinent question regarding mechanism of autophagy regulation by ESAT-6. Current opinions in the field of mycobacterial pathogenesis highlight the decisive role of miRNA in regulating host immune responses, disease progression and effector functions like apoptosis and autophagy.[50,51,77] Positive or negative regulation of autophagy by miRNA in mycobacteria infected cells led us to speculate that mycobacterial antigen like ESAT-6 may have a protective potency to dampen the autophagic response through miRNA to lend survival advantage to the invading pathogen. The expression of few miRNAs like miR-17-5p, miR-30a, miR-33, miR-125a-3p, miR-144 and miR-3619-5p have already been reported to be altered by the mycobacterial species that affected autophagic response, but the interplay of ESAT-6 in this modulation is not at all known to the best of our knowledge.[51,52,58–60,84] Hence, we next looked at the regulation of these miRNAs by rESAT-6 and its repercussions on the Calcimycin-induced autophagy and intracellular growth of the mycobacteria. In our experimental setting, we observed differential expression of above-listed miRNAs by approx. 0.7–5.5 fold upon Calcimycin treatment. Interestingly, rESAT-6 only modulated the expression of miR-30a-3p and miR-30a-5p antagonistically that led us to strongly believe that these microRNAs may have a potential role in altering the autophagy induced by Calcimycin in dTHP-1 cells. Our findings are also coherent with the recent reports where miR-30 family members have been shown to regulate different disease pathologies and development of tissues and organs.[53,85–89] The observed opposing modulation like inhibition or activation of miR-30a-5p or miR-30a-3p expression by rESAT-6 is in line with the growing hypothesis that both arms of a mature miRNAs, 3p and 5p play an important role in the gene regulation and can have opposing functions as well.[90,91] Paradoxical regulation of miR-30a-3p and miR-30a-5p by rESAT-6 also led us to hypothesize the presence of some molecular switch acting as a master regulator of these miRNAs that warrants future investigation in greater detail. Association of miR-30a-3p and miR-30a-5p with Calcimycin-induced autophagy was further explored using specific mimics or inhibitors against these miRNAs. Transfection experiments conclusively prove the role of miR-30a-5p in Calcimycin-induced autophagy and miR-30a-3p in rESAT-6 mediated autophagy inhibition. Suppression of either miR-30a-5p or miR-30a-3p miRNA aborted the effects of Calcimycin or rESAT-6 respectively on the intracellular growth of mycobacteria, thus supporting the emerging concept of utilizing miRNA in HDT for better understanding the control mechanisms manifested by the host against mycobacteria.

For futuristic studies, it would be pertinent to perform miRNA expression profiling in Calcimycin-treated cells with or without rESAT-6 pre-treatment to identify novel miRNA molecules that may have the potential to affect TB biology leading to better control and management of this disease. Understanding the mechanistic regulation of miRNA expression in our experimental setting for future will also help in designing novel TB therapeutics. Furthermore, bioinformatics analysis of the putative binding sites of miR-30a-3p, miR-30a-5p or another miRNA at 3′-UTR of the host target will aid to delineate the mechanistic regulation of autophagy by miRNAs that will help to ascertain its application and relevance in fostering efficacy of either first-line anti tubercular drugs or TB vaccines. In last decade, many experimental findings have validated targets of miR-30a in host like Beclin-1, Atg 5, MyD88, Yin-Yang 1 (YY1), Sirtuin 1 (SIRT1) etc. in different diseases[53,56,88,92–94] but their role in our experimental setting to regulate autophagy for the time being is a matter of conjecture and warrants further detailed investigation.

In conclusion, our study for the first time has unraveled the mechanistic regulation of the miRNAs by rESAT-6 that helps in providing favorable niche to the intracellular bacteria for its survival by modulating processes such as autophagy. The contrasting roles of the two miRNAs originating from the same pre-miRNA also revealed the intricacies of this modulation that needs to be investigated in greater depth in future for designing effective strategies against TB. Taken together, this is the first study, where we show that the two arms of same microRNA are differentially regulated by ESAT-6 to affect mycobacterial survival by modulating autophagy.

Acknowledgments

We thank Dr. Vivek Rai, (Institute of Life Science, Bhubaneswar, India) for providing THP-1 cell-line. We are grateful to Dr. Manjula Kalia (Regional Centre for Biotechnology, Faridabad, Haryana, India) and Dr. Sujit K. Bhutia (Department of Life Science, NIT Rourkela) for sharing ptf-LC3 plasmid. Help extended by Dr. Dhiraj Kumar, International Centre for Genetic Engineering and Biotechnology, New Delhi in sharing wild type *M. tb* H37Rv and *M. tb* H37Rv Δ ESAT-6 strains is greatly acknowledged. We also thank to the help extended by Dr. Vidya D. Negi and her group along with faculties of Department of Life Science, NIT Rourkela. Contribution of Dr. Ramakrishna Vankayalapati (University of Texas Health Science Center at Tyler, Texas, USA) for providing critical inputs during the preparation of this manuscript is also acknowledged. We thank Mr. Sushanth Pradhan from Biotechnology and Medical Engineering department, NIT Rourkela for the support in executing confocal microscopy work.

Conflict of interest

The authors have no conflict of interest to declare related to this article.

Funding

Department of Science and Technology (DST), Govt. of India (EMR/2016/000048, EEQ/2016/000205 and DST/INSPIRE/Faculty award/2014/DST/INSPIRE/04/2014/01662) is acknowledged by RD for the generous financial support. RD is also thankful to the Ministry of Human Resource and Development (MHRD), Govt. of India for intramural support. Financial support provided to RS by DST, Govt. of India (EMR/2015/000426) and THSTI is also acknowledged. RS is a recipient of National Bioscience award and Ramalingaswami fellowship. The research fellowship by DST to AB, MHRD to AM, SM and AK and the Council of Scientific and Industrial Research (CSIR), Govt. of India to SG is deeply acknowledged. DM is thankful to DST for Kishore Vaigyanik Protsahan Yojana (KVPY) fellowship.

Supplementary materials

Supplementary material associated with this article can be found, in the online version, at doi:10.1016/j.jinf.2019.06.001.

References

1. World Health Organization. *Global tuberculosis report 2018*. Geneva, Switzerland: World Health Organization; 2018 https://www.who.int/tb/publications/global_report/en/External.

2. Andersen P, Doherty TM. The success and failure of BCG – implications for a novel tuberculosis vaccine. *Nat Rev Microbiol* 2005;**3**(8):656–62 PubMed PMID:16012514.
3. Brandt L, Feino Cunha J, Weinreich Olsen A, Chilima B, Hirsch P, Appelberg R, et al. Failure of the Mycobacterium bovis BCG vaccine: some species of environmental mycobacteria block multiplication of BCG and induction of protective immunity to tuberculosis. *Infect Immun* 2002;**70**(2):672–8 PubMed PMID:11796598 Pubmed Central PMCID: 127715.
4. Getahun H, Chaisson RE, Raviglione M. Latent Mycobacterium tuberculosis Infection. *N Engl J Med* 2015;**373**(12):1179–80 PubMed PMID:26376149.
5. Modlin RL, Bloom BR. TB or not TB: that is no longer the question. *Sci Transl Med* 2013;**5**(213):213sr6 PubMed PMID:24285487.
6. Collins HL, Kaufmann SH. The many faces of host responses to tuberculosis. *Immunology* 2001;**103**(1):1–9 PubMed PMID:11380686 Pubmed Central PMCID: 1783212.
7. Flynn JL, Chan J. Immunology of tuberculosis. *Ann Rev Immunol* 2001;**19**:93–129 PubMed PMID:11244032.
8. Khan A, Jagannath C. Analysis of host-pathogen modulators of autophagy during Mycobacterium tuberculosis infection and therapeutic repercussions. *Int Rev Immunol* 2017;**36**(5):271–86 PubMed PMID:28976784.
9. Songane M, Kleinnijenhuis J, Netea MG, van Crevel R. The role of autophagy in host defence against Mycobacterium tuberculosis infection. *Tuberculosis* 2012;**92**(5):388–96 PubMed PMID:22683183Epub 2012/06/12. eng.
10. Torrado E, Cooper AM. Cytokines in the balance of protection and pathology during mycobacterial infections. *Adv Exp Med Biol* 2013;**783**:121–40 PubMed PMID:23468107 Pubmed Central PMCID: 3773506.
11. Levine B, Kroemer G. Autophagy in the pathogenesis of disease. *Cell* 2008;**132**(1):27–42 PubMed PMID:18191218 Pubmed Central PMCID: 2696814. Epub 2008/01/15. eng.
12. Wang CW, Klionsky DJ. The molecular mechanism of autophagy. *Mol Med* 2003;**9**(3–4):65–76 PubMed PMID:12865942 Pubmed Central PMCID: 1430730. Epub 2003/07/17. eng.
13. Dikic I, Elazar Z. Mechanism and medical implications of mammalian autophagy. *Nat Rev Mol Cell Biol* 2018;**19**(6):349–64 PubMed PMID:29618831.
14. Mizushima N. A brief history of autophagy from cell biology to physiology and disease. *Nat Cell Biol* 2018;**20**(5):521–7 PubMed PMID:29686264.
15. Saha S, Panigrahi DP, Patil S, Bhutia SK. Autophagy in health and disease: a comprehensive review. *Biomed Pharmacother (Biomedecine & Pharmacotherapie)* 2018;**104**:485–95 PubMed PMID:29800913.
16. Deretic V. Autophagy in immunity and cell-autonomous defense against intracellular microbes. *Immunol Rev* 2011;**240**(1):92–104 PubMed PMID:21349088 Pubmed Central PMCID: 3057454.
17. Desai M, Fang R, Sun J. The role of autophagy in microbial infection and immunity. *ImmunoTargets Ther* 2015;**4**:13–26 PubMed PMID:27471708 Pubmed Central PMCID: 4918246.
18. Levine B, Mizushima N, Virgin HW. Autophagy in immunity and inflammation. *Nature* 2011;**469**(7330):323–35 PubMed PMID:21248839 Pubmed Central PMCID: 3131688.
19. Pengo N, Scolari M, Oliva L, Milan E, Mainoldi F, Raimondi A, et al. Plasma cells require autophagy for sustainable immunoglobulin production. *Nature Immunol* 2013;**14**(3):298–305 PubMed PMID:23354484.
20. Deretic V, Levine B. Autophagy, immunity, and microbial adaptations. *Cell Host Microbe* 2009;**5**(6):527–49 PubMed PMID:19527881 Pubmed Central PMCID: 2720763.
21. Levine B. Eating oneself and uninvited guests: autophagy-related pathways in cellular defense. *Cell* 2005;**120**(2):159–62 PubMed PMID:15680321.
22. Walker DH, Popov VL, Crocquet-Valdes PA, Welsh CJ, Feng HM. Cytokine-induced, nitric oxide-dependent, intracellular antirickettsial activity of mouse endothelial cells. *Lab Investig J Tech Methods Pathol* 1997;**76**(1):129–38 PubMed PMID:9010456.
23. Mawatwal S, Behura A, Ghosh A, Kidwai S, Mishra A, Deep A, et al. Calcimycin mediates mycobacterial killing by inducing intracellular calcium-regulated autophagy in a P2RX7 dependent manner. *Biochim Biophys Acta* 2017;**1861**(12):3190–200 PubMed PMID:28935606.
24. Mawatwal S, Behura A, Mishra A, Singh R, Dhiman R. Calcimycin induced IL-12 production inhibits intracellular mycobacterial growth by enhancing autophagy. *Cytokine* 2018;**111**:1–12 PubMed PMID:30081297.
25. Liang M, Habib Z, Sakamoto K, Chen X, Cao G. Mycobacteria and autophagy: many questions and few answers. *Curr Issues Mol Biol* 2017;**21**:63–72 PubMed PMID:27443861.
26. Condos R, Raju B, Canova A, Zhao BY, Weiden M, Rom WN, et al. Recombinant gamma interferon stimulates signal transduction and gene expression in alveolar macrophages in vitro and in tuberculosis patients. *Infect Immun* 2003;**71**(4):2058–64 PubMed PMID:12654826 Pubmed Central PMCID: 152019.
27. Freeman S, Post FA, Bekker LG, Harbacheuski R, Steyn LM, Ryffel B, et al. Mycobacterium tuberculosis H37Ra and H37Rv differential growth and cytokine/chemokine induction in murine macrophages in vitro. *J Interferon Cytokine Res Off J Int Soc Interferon Cytokine Res* 2006;**26**(1):27–33 PubMed PMID:16426145.
28. Harris J, De Haro SA, Master SS, Keane J, Roberts EA, Delgado M, et al. T helper 2 cytokines inhibit autophagic control of intracellular Mycobacterium tuberculosis. *Immunity* 2007;**27**(3):505–17 PubMed PMID:17892853.
29. Harris J, Master SS, De Haro SA, Delgado M, Roberts EA, Hope JC, et al. Th1–Th2 polarisation and autophagy in the control of intracellular mycobacteria by macrophages. *Vet Immunol Immunopathol* 2009;**128**(1–3):37–43 PubMed PMID:19026454 Pubmed Central PMCID: 2789833.
30. Thompson CR, Iyer SS, Melrose N, VanOosten R, Johnson K, Pitson SM, et al. Sphingosine kinase 1 (SK1) is recruited to nascent phagosomes in human macrophages: inhibition of SK1 translocation by Mycobacterium tuberculosis. *J Immunol* 2005;**174**(6):3551–61 PubMed PMID:15749892.
31. Yadav M, Clark L, Schorey JS. Macrophage's proinflammatory response to a mycobacterial infection is dependent on sphingosine kinase-mediated activation of phosphatidylinositol phospholipase C, protein kinase C, ERK1/2, and phosphatidylinositol 3-kinase. *J Immunol* 2006;**176**(9):5494–503 PubMed PMID:16622018.
32. Dutta RK, Kathania M, Raje M, Majumdar S. IL-6 inhibits IFN-gamma induced autophagy in Mycobacterium tuberculosis H37Rv infected macrophages. *Int J Biochem Cell Biol* 2012;**44**(6):942–54 PubMed PMID:22426116.
33. Chandra P, Ghanwat S, Matta SK, Yadav SS, Mehta M, Siddiqui Z, et al. Mycobacterium tuberculosis Inhibits RAB7 recruitment to selectively modulate autophagy flux in macrophages. *Sci Rep* 2015;**5**:16320 PubMed PMID:26541268 Pubmed Central PMCID: 4635374.
34. Duan L, Yi M, Chen J, Li S, Chen W. Mycobacterium tuberculosis Eis gene inhibits macrophage autophagy through up-regulation of IL-10 by increasing the acetylation of histone H3. *Biochem Biophys Res Commun* 2016;**473**(4):1229–34 PubMed PMID:27079235.
35. Shin DM, Jeon BY, Lee HM, Jin HS, Yuk JM, Song CH, et al. Mycobacterium tuberculosis Eis regulates autophagy, inflammation, and cell death through redox-dependent signaling. *PLoS Pathog* 2010;**6**(12):e1001230 PubMed PMID:21187903 Pubmed Central PMCID: 3002989.
36. Shui W, Petzold CJ, Redding A, Liu J, Pitcher A, Sheu L, et al. Organelle membrane proteomics reveals differential influence of mycobacterial lipoglycans on macrophage phagosome maturation and autophagosome accumulation. *J Proteome Res* 2011;**10**(1):339–48 PubMed PMID:21105745 Pubmed Central PMCID: 3018347.
37. Romagnoli A, Etna MP, Giacomini E, Pardini M, Remoli ME, Corazzari M, et al. ESX-1 dependent impairment of autophagic flux by Mycobacterium tuberculosis in human dendritic cells. *Autophagy* 2012;**8**(9):1357–70 PubMed PMID:22885411 Pubmed Central PMCID: 3442882.
38. Bach H, Papavinasasundaram KG, Wong D, Hmama Z, Av-Gay Y. Mycobacterium tuberculosis virulence is mediated by PtpA dephosphorylation of human vacuolar protein sorting 33B. *Cell Host Microbe.* 2008;**3**(5):316–22 PubMed PMID:18474358.
39. Singh R, Rao V, Shakila H, Gupta R, Khera A, Dhar N, et al. Disruption of mptpB impairs the ability of Mycobacterium tuberculosis to survive in guinea pigs. *Mol Microbiol* 2003;**50**(3):751–62 PubMed PMID:14617138.
40. Wong KW. The role of ESX-1 in Mycobacterium tuberculosis pathogenesis. *Microbiol Spectr* 2017;**5**(3) TBTB2-0001-2015, PubMed PMID:28513416.
41. Behr MA, Wilson MA, Gill WP, Salamon H, Schoolnik GK, Rane S, et al. Comparative genomics of BCG vaccines by whole-genome DNA microarray. *Science* 1999;**284**(5419):1520–3 PubMed PMID:10348738.
42. Hsu T, Hingley-Wilson SM, Chen B, Chen M, Dai AZ, Morin PM, et al. The primary mechanism of attenuation of bacillus Calmette–Guerin is a loss of secreted lytic function required for invasion of lung interstitial tissue. *Proc Natl Acad Sci USA* 2003;**100**(21):12420–5 PubMed PMID:14557547 Pubmed Central PMCID: 218773.
43. Lewis KN, Liao R, Guinn KM, Hickey MJ, Smith S, Behr MA, et al. Deletion of RD1 from Mycobacterium tuberculosis mimics bacille Calmette–Guerin attenuation. *J Infect Dis* 2003;**187**(1):117–23 PubMed PMID:12508154 Pubmed Central PMCID: 1458498.
44. Pym AS, Brodin P, Brosch R, Huerre M, Cole ST. Loss of RD1 contributed to the attenuation of the live tuberculosis vaccines Mycobacterium bovis BCG and Mycobacterium microti. *Mol Microbiol* 2002;**46**(3):709–17 PubMed PMID:12410828.
45. Abdallah AM, Gey van Pittius NC, Champion PA, Cox J, Luirink J, Vandenbroucke-Grauls CM, et al. Type VII secretion–mycobacteria show the way. *Nat Rev Microbiol* 2007;**5**(11):883–91 PubMed PMID:17922044.
46. Peng X, Sun J. Mechanism of ESAT-6 membrane interaction and its roles in pathogenesis of Mycobacterium tuberculosis. *Toxicon: Off J Int Soc Toxinol* 2016;**116**:29–34 PubMed PMID:26456678 Pubmed Central PMCID: 4973572.
47. Watson RO, Manzanillo PS, Cox JS. Extracellular M. tuberculosis DNA targets bacteria for autophagy by activating the host DNA-sensing pathway. *Cell* 2012;**150**(4):803–15 PubMed PMID:22901810 Pubmed Central PMCID: 3708656.
48. Dong H, Jing W, Runpeng Z, Xuewei X, Min M, Ru C, et al. ESAT6 inhibits autophagy flux and promotes BCG proliferation through MTOR. *Biochem Biophys Res Commun* 2016;**477**(2):195–201 PubMed PMID:27317487.
49. Kumar R, Halder P, Sahu SK, Kumar M, Kumari M, Jana K, et al. Identification of a novel role of ESAT-6-dependent miR-155 induction during infection of macrophages with Mycobacterium tuberculosis. *Cell Microbiol* 2012;**14**(10):1620–31 PubMed PMID:22712528.
50. Yang T, Ge B. miRNAs in immune responses to Mycobacterium tuberculosis infection. *Cancer Lett* 2018;**431**:22–30 PubMed PMID:29803788.
51. Kim JK, Kim TS, Basu J, Jo EK. MicroRNA in innate immunity and autophagy during mycobacterial infection. *Cell Microbiol* 2017;**19**(1) PubMed PMID:27794209.
52. Das K, Garnica O, Dhandayuthapani S. Modulation of host miRNAs by intracellular bacterial pathogens. *Front Cell Infect Microbiol* 2016;**6**:79 PubMed PMID:27536558 Pubmed Central PMCID: 4971075.
53. Mao L, Liu S, Hu L, Jia L, Wang H, Guo M, et al. miR-30 Family: a promising regulator in development and disease. *BioMed Res Int* 2018;**2018**:9623412 PubMed PMID:30003109 Pubmed Central PMCID: 5996469.
54. Chen Z, Wang T, Liu Z, Zhang G, Wang J, Feng S, et al. Inhibition of autophagy by MiR-30A induced by mycobacteria tuberculosis as a possible mechanism of

immune escape in human macrophages. *Jpn J Infect Dis* 2015;**68**(5):420–4 PubMed PMID:25866116.
55. Liu Z, Zhou G, Deng X, Yu Q, Hu Y, Sun H, et al. Analysis of miRNA expression profiling in human macrophages responding to Mycobacterium infection: induction of the immune regulator miR-146a. *J Infect* 2014;**68**(6):553–61 PubMed PMID:24462562.
56. Wu Y, Sun Q, Dai L. Immune regulation of miR-30 on the Mycobacterium tuberculosis-induced TLR/MyD88 signaling pathway in THP-1 cells. *Exp Ther Med* 2017;**14**(4):3299–303 PubMed PMID:28912881 Pubmed Central PMCID: 5585754.
57. Liu F, Chen J, Wang P, Li H, Zhou Y, Liu H, et al. MicroRNA-27a controls the intracellular survival of Mycobacterium tuberculosis by regulating calcium-associated autophagy. *Nat Commun* 2018;**9**(1):4295 PubMed PMID:30327467 Pubmed Central PMCID: 6191460.
58. Kim JK, Lee HM, Park KS, Shin DM, Kim TS, Kim YS, et al. MIR144* inhibits antimicrobial responses against Mycobacterium tuberculosis in human monocytes and macrophages by targeting the autophagy protein DRAM2. *Autophagy* 2017;**13**(2):423–41 PubMed PMID:27764573 Pubmed Central PMCID: 5324854.
59. Kumar R, Sahu SK, Kumar M, Jana K, Gupta P, Gupta UD, et al. MicroRNA 17-5p regulates autophagy in Mycobacterium tuberculosis-infected macrophages by targeting Mcl-1 and STAT3. *Cell Microbiol* 2016;**18**(5):679–91 PubMed PMID:26513648.
60. Ouimet M, Koster S, Sakowski E, Ramkhelawon B, van Solingen C, Oldebeken S, et al. Mycobacterium tuberculosis induces the miR-33 locus to reprogram autophagy and host lipid metabolism. *Nat Immunol* 2016;**17**(6):677–86 PubMed PMID:27089382 Pubmed Central PMCID: 4873392.
61. Liu Y, Wang R, Jiang J, Yang B, Cao Z, Cheng X. miR-223 is upregulated in monocytes from patients with tuberculosis and regulates function of monocyte-derived macrophages. *Mol Immunol* 2015;**67**(2 Pt B):475–81 PubMed PMID:26296289.
62. Iwai H, Funatogawa K, Matsumura K, Kato-Miyazawa M, Kirikae F, Kiga K, et al. MicroRNA-155 knockout mice are susceptible to Mycobacterium tuberculosis infection. *Tuberculosis* 2015;**95**(3):246–50 PubMed PMID:25846955.
63. Dhiman R, Raje M, Majumdar S. Differential expression of NF-kappaB in mycobacteria infected THP-1 affects apoptosis. *Biochim Biophys Acta* 2007;**1770**(4):649–58 PubMed PMID:17204371.
64. Singh R, Singh M, Arora G, Kumar S, Tiwari P, Kidwai S. Polyphosphate deficiency in Mycobacterium tuberculosis is associated with enhanced drug susceptibility and impaired growth in guinea pigs. *J Bacteriol* 2013;**195**(12):2839–51 PubMed PMID:23585537 Pubmed Central PMCID: 3697247.
65. Abdalla AE, Lambert N, Duan X, Xie J. Interleukin-10 family and tuberculosis: an old story renewed. *Int J Biol Sci* 2016;**12**(6):710–17 PubMed PMID:27194948 Pubmed Central PMCID: 4870714.
66. Boussiotis VA, Freeman GJ, Taylor PA, Berezovskaya A, Grass I, Blazar BR, et al. p27kip1 functions as an anergy factor inhibiting interleukin 2 transcription and clonal expansion of alloreactive human and mouse helper T lymphocytes. *Nat Med* 2000;**6**(3):290–7 PubMed PMID:10700231.
67. Sharifi MN, Mowers EE, Drake LE, Macleod KF. Measuring autophagy in stressed cells. *Methods Mol Biol* 2015;**1292**:129–50 PubMed PMID:25804753 Pubmed Central PMCID: 4460991.
68. Mizushima N, Yoshimori T. How to interpret LC3 immunoblotting. *Autophagy* 2007;**3**(6):542–5 PubMed PMID:17611390.
69. Mauvezin C, Neufeld TP. Bafilomycin A1 disrupts autophagic flux by inhibiting both V-ATPase-dependent acidification and Ca-P60A/SERCA-dependent autophagosome-lysosome fusion. *Autophagy* 2015;**11**(8):1437–8 PubMed PMID:26156798 Pubmed Central PMCID: 4590655.
70. Kimura S, Noda T, Yoshimori T. Dissection of the autophagosome maturation process by a novel reporter protein, tandem fluorescent-tagged LC3. *Autophagy* 2007;**3**(5):452–60 PubMed PMID:17534139.
71. Lofthouse EK, Wheeler PR, Beste DJ, Khatri BL, Wu H, Mendum TA, et al. Systems-based approaches to probing metabolic variation within the Mycobacterium tuberculosis complex. *PloS One* 2013;**8**(9):e75913 PubMed PMID:24098743 Pubmed Central PMCID: 3783153.
72. Paul P, Chakraborty A, Sarkar D, Langthasa M, Rahman M, Bari M, et al. Interplay between miRNAs and human diseases. *J Cell Physiol* 2018;**233**(3):2007–18 PubMed PMID:28181241.
73. Lee RC, Feinbaum RL, Ambros V. The C. elegans heterochronic gene lin-4 encodes small RNAs with antisense complementarity to lin-14. *Cell* 1993;**75**(5):843–54 PubMed PMID:8252621.
74. Gebert LFR, MacRae IJ. Regulation of microRNA function in animals. *Nat Rev Mol Cell Biol* 2018 PubMed PMID:30108335.
75. Pallez D, Gardes J, Pasquier C. Prediction of miRNA-disease associations using an evolutionary tuned latent semantic analysis. *Sci Rep* 2017;**7**(1):10548 PubMed PMID:28874691 Pubmed Central PMCID: 5585369.
76. Staedel C, Darfeuille F. MicroRNAs and bacterial infection. *Cell Microbiol* 2013;**15**(9):1496–507 PubMed PMID:23795564.
77. Sabir N, Hussain T, Shah SZA, Peramo A, Zhao D, Zhou X. miRNAs in tuberculosis: new avenues for diagnosis and host-directed therapy. *Front Microbiol* 2018;**9**:602 PubMed PMID:29651283 Pubmed Central PMCID: 5885483.
78. Ni B, Rajaram MV, Lafuse WP, Landes MB, Schlesinger LS. Mycobacterium tuberculosis decreases human macrophage IFN-gamma responsiveness through miR-132 and miR-26a. *J Immunol* 2014;**193**(9):4537–47 PubMed PMID:25252958.
79. Ganguly N, Siddiqui I, Sharma P. Role of M. tuberculosis RD-1 region encoded secretory proteins in protective response and virulence. *Tuberculosis* 2008;**88**(6):510–17 PubMed PMID:18640874.
80. Skjot RL, Oettinger T, Rosenkrands I, Ravn P, Brock I, Jacobsen S, et al. Comparative evaluation of low-molecular-mass proteins from Mycobacterium tuberculosis identifies members of the ESAT-6 family as immunodominant T-cell antigens. *Infect Immun* 2000;**68**(1):214–20 PubMed PMID:10603390 Pubmed Central PMCID: 97123.
81. Brodin P, Rosenkrands I, Andersen P, Cole ST, Brosch R. ESAT-6 proteins: protective antigens and virulence factors? *Trends Microbiol* 2004;**12**(11):500–8 PubMed PMID:15488391.
82. Zhang L, Zhang H, Zhao Y, Mao F, Wu J, Bai B, et al. Effects of Mycobacterium tuberculosis ESAT-6/CFP-10 fusion protein on the autophagy function of mouse macrophages. *DNA Cell Biol* 2012;**31**(2):171–9 PubMed PMID:21740189.
83. Renshaw PS, Lightbody KL, Veverka V, Muskett FW, Kelly G, Frenkiel TA, et al. Structure and function of the complex formed by the tuberculosis virulence factors CFP-10 and ESAT-6. *EMBO J* 2005;**24**(14):2491–8 PubMed PMID:15973432 Pubmed Central PMCID: 1176459.
84. Kim JK, Yuk JM, Kim SY, Kim TS, Jin HS, Yang CS, et al. MicroRNA-125a inhibits autophagy activation and antimicrobial responses during mycobacterial infection. *J Immunol* 2015;**194**(11):5355–65 PubMed PMID:25917095.
85. Liu QY, Chang MN, Lei JX, Koukiekolo R, Smith B, Zhang D, et al. Identification of microRNAs involved in Alzheimer's progression using a rabbit model of the disease. *Am J Neurodegener Dis* 2014;**3**(1):33–44 PubMed PMID:24754001 Pubmed Central PMCID: 3986609.
86. Wu G, Yang G, Zhang R, Xu G, Zhang L, Wen W, et al. Altered microRNA expression profiles of extracellular vesicles in nasal mucus from patients with allergic rhinitis. *Allergy Asthma Immunol Res* 2015;**7**(5):449–57 PubMed PMID:26122505 Pubmed Central PMCID: 4509657.
87. Liu X, Ji Q, Zhang C, Liu X, Liu Y, Liu N, et al. miR-30a acts as a tumor suppressor by double-targeting COX-2 and BCL9 in H. pylori gastric cancer models. *Sci Rep* 2017;**7**(1):7113 PubMed PMID:28769030 Pubmed Central PMCID: 5540978.
88. Jiang LH, Zhang HD, Tang JH. MiR-30a: a novel biomarker and potential therapeutic target for cancer. *J Oncol* 2018;**2018**:5167829 PubMed PMID:30158978 Pubmed Central PMCID: 6106977.
89. Yang SJ, Yang SY, Wang DD, Chen X, Shen HY, Zhang XH, et al. The miR-30 family: versatile players in breast cancer. *Tumour Biol J Int Soc Oncodevelopmental Biol Med* 2017;**39**(3):1010428317692204 PubMed PMID:28347244.
90. Ren LL, Yan TT, Shen CQ, Tang JY, Kong X, Wang YC, et al. The distinct role of strand-specific miR-514b-3p and miR-514b-5p in colorectal cancer metastasis. *Cell Death Dis* 2018;**9**(6):687 PubMed PMID:29880874 Pubmed Central PMCID: 5992212.
91. Yang X, Du WW, Li H, Liu F, Khorshidi A, Rutnam ZJ, et al. Both mature miR-17-5p and passenger strand miR-17-3p target TIMP3 and induce prostate tumor growth and invasion. *Nucleic Acids Res* 2013;**41**(21):9688–704 PubMed PMID:23990326 Pubmed Central PMCID: 3834805.
92. Guan Y, Rao Z, Chen C. miR-30a suppresses lung cancer progression by targeting SIRT1. *Oncotarget* 2018;**9**(4):4924–34 PubMed PMID:29435152 Pubmed Central PMCID: 5797023.
93. Yang C, Zhang JJ, Peng YP, Zhu Y, Yin LD, Wei JS, et al. A Yin-Yang 1/miR-30a regulatory circuit modulates autophagy in pancreatic cancer cells. *J Transl Med* 2017;**15**(1):211 PubMed PMID:29052509 Pubmed Central PMCID: 5649049.
94. Yu Y, Yang L, Zhao M, Zhu S, Kang R, Vernon P, et al. Targeting microRNA-30a-mediated autophagy enhances imatinib activity against human chronic myeloid leukemia cells. *Leukemia* 2012;**26**(8):1752–60 PubMed PMID:22395361.